Radiative-Recoil Corrections in Muonium and Positronium

Greg Adkins
Franklin & Marshall College
Lancaster, Pennsylvania, USA
18 May 2026

Radiative-Recoil Corrections in Muonium and Positronium

- Motivation
- Experimental Situation
- Method of Calculation
- Results
- Conclusion

Student Collaborators:
Addison Kovats-Bernat
Elias Mitchell
Volkan Turan

Acknowledgments
NSF PHY-2308792
NIST 60NANB23D230
Franklin & Marshall College

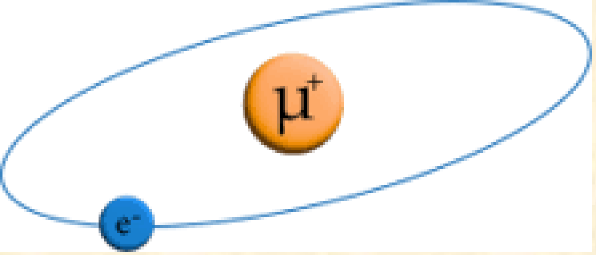

Muonium: a purely leptonic exotic atom

Muonium, the μ^+e^- bound system, is closely analogous to hydrogen but with several important differences. First, both of it's constituents are structureless point-like particles. Compared to hydrogen, where the proton size and internal structure matter, the theoretical analysis of muonium is relatively straightforward. Recoil effects are more important in muonium than in hydrogen, given that m_e/m_μ=1/207 while m_e/m_p=1/1837. The finite muon lifetime of τ=2.2 μs leads to a natural minimum linewidth through the uncertainty principle.

High precision measurements of many of the muonium n=1 and n=2 transitions combined with the possibility of high precision calculation of those transition frequencies based mainly on QED make muonium an attractive system for the determination of fundamental constants and testing the limits of current theory.

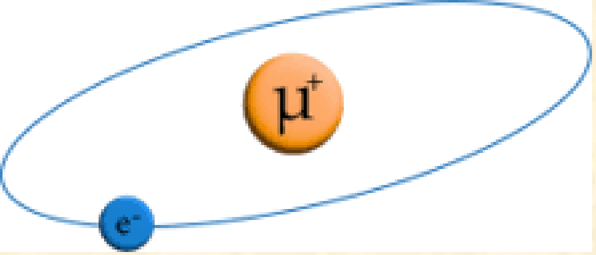

Muonium Spectrum

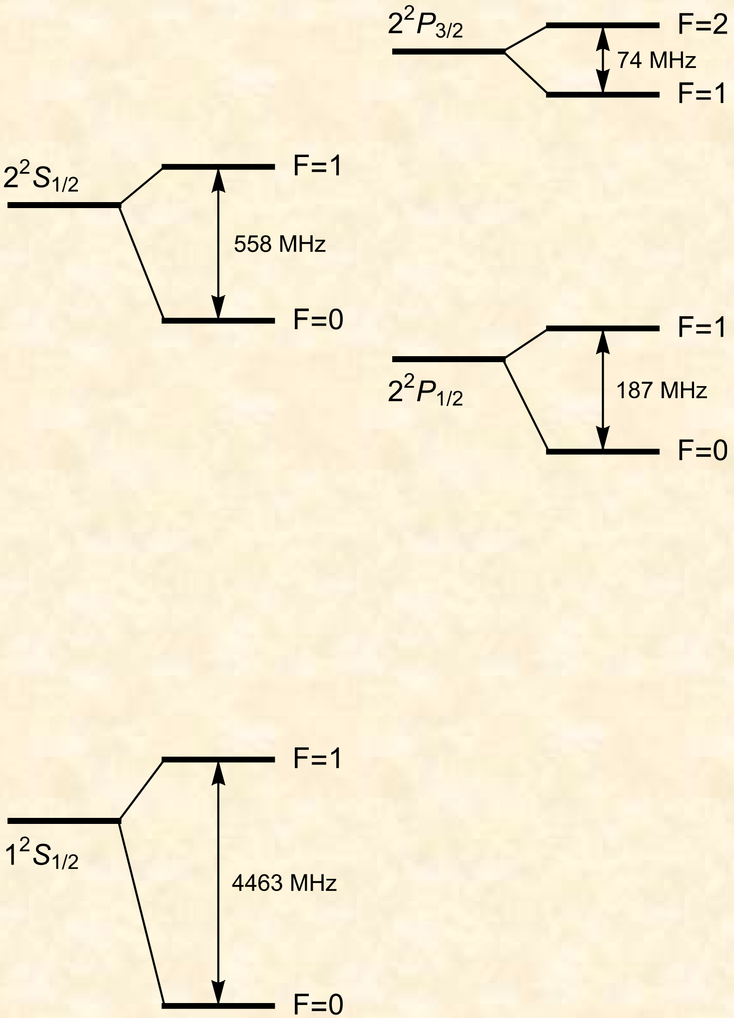

The n=1 and n=2 muonium energy levels are shown, along with the hyperfine intervals.

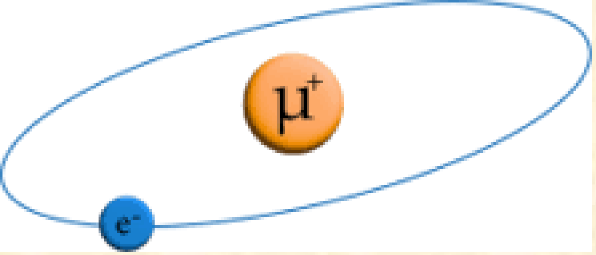

Muonium Spectrum

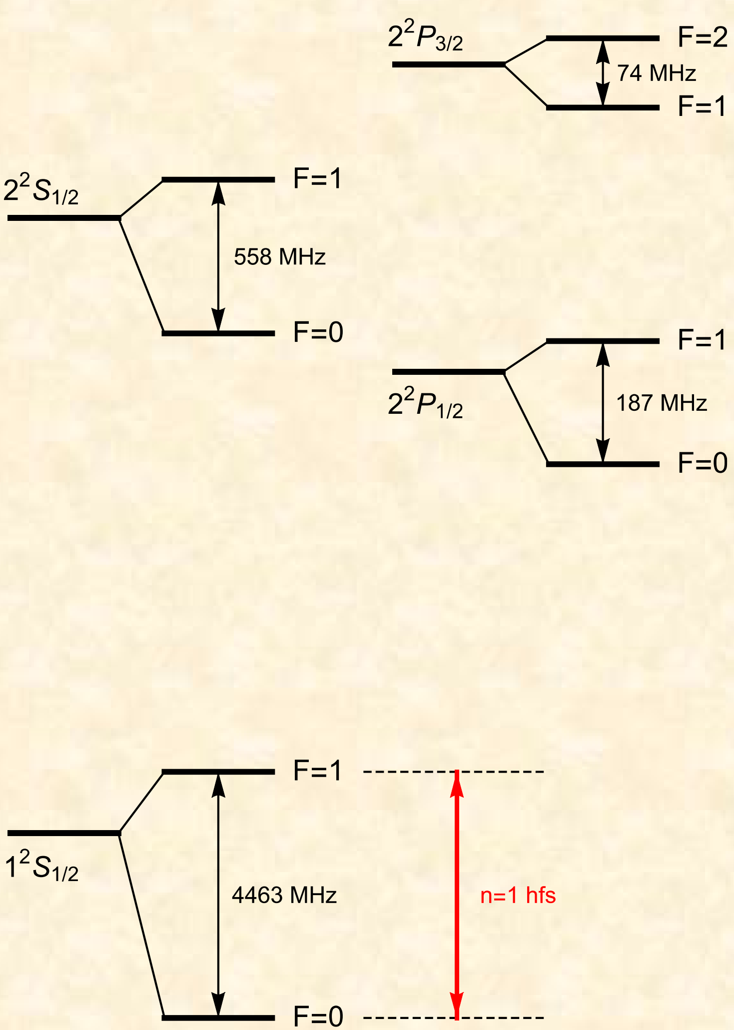

The n=1 hyperfine interval has been measured to high precision:

$$\Delta E = 4\,463\,302.88(16)\,\mathrm{kHz}$$

F.G.Marion et al., Phys. Rev. Lett. 49, 993 (1982)

$$\Delta E = 4\,463\,302.765(53)\,\mathrm{kHz}$$

W.Liu et al., Phys. Rev. Lett. 82, 711 (1999)

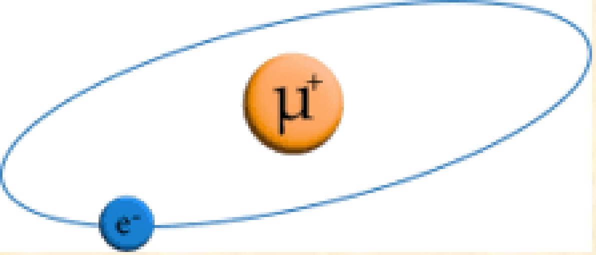

Muonium Spectrum

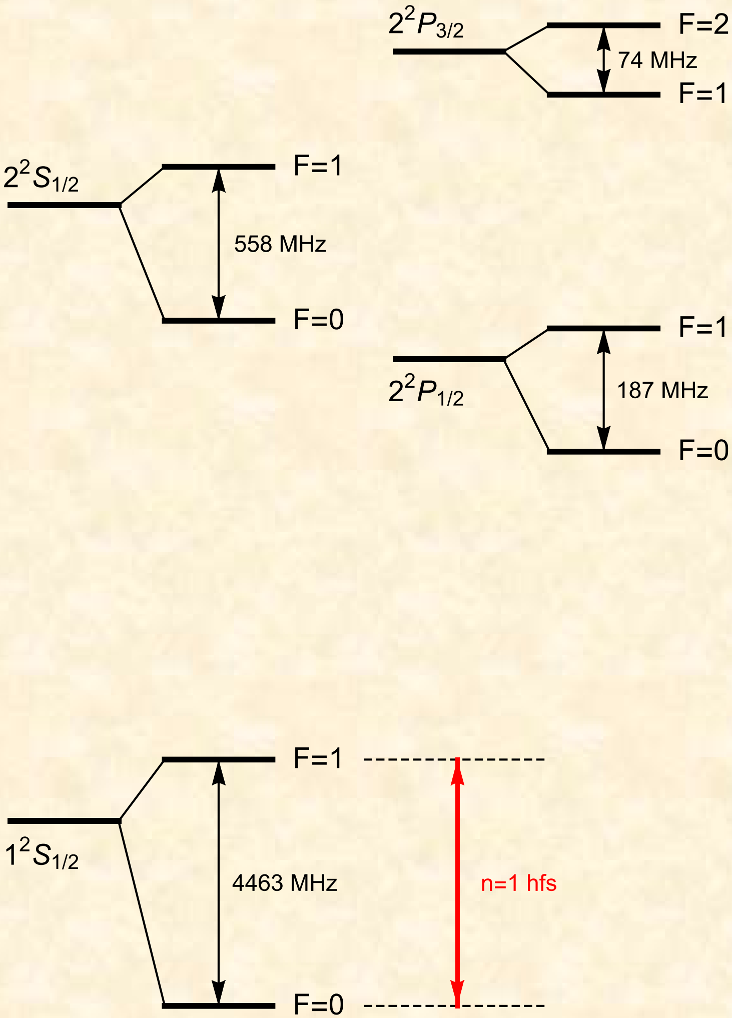

The n=1 hyperfine interval has been measured to high precision:

$$\Delta E = 4\,463\,302.88(16)\,\mathrm{kHz}$$

F.G.Marion et al., Phys. Rev. Lett. 49, 993 (1982)

$$\Delta E = 4\,463\,302.765(53)\,\mathrm{kHz}$$

W.Liu et al., Phys. Rev. Lett. 82, 711 (1999)

$$\Delta E = 4\,463\,302(4)\,\mathrm{kHz}$$

S.Kanda et al. (MuSEUM), Phys. Lett. B 815, 136154 (2021)

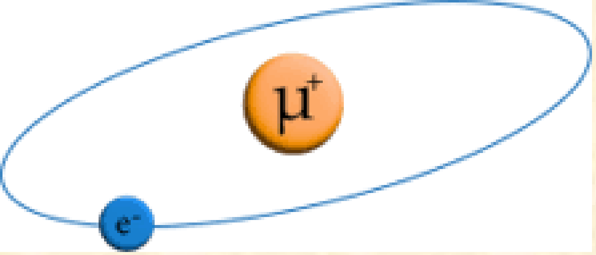

Muonium Spectrum

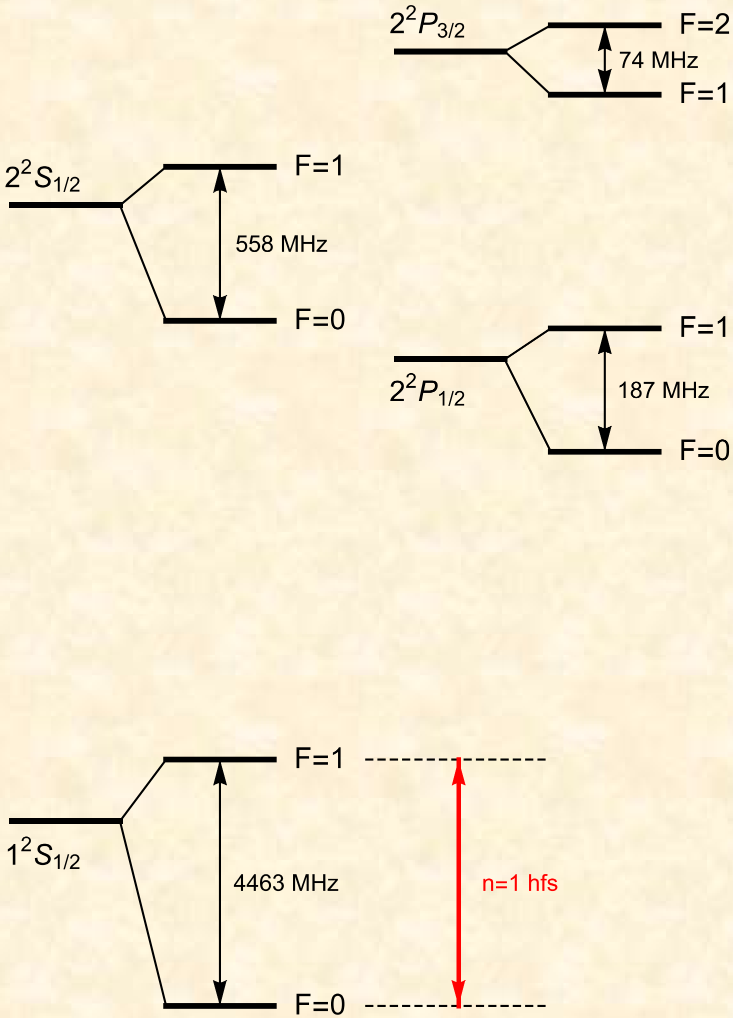

The n=1 hyperfine interval has been measured to high precision:

$$\Delta E = 4\,463\,302.88(16)\,\mathrm{kHz}$$

F.G.Marion et al., Phys. Rev. Lett. 49, 993 (1982)

$$\Delta E = 4\,463\,302.765(53)\,\mathrm{kHz}$$

W.Liu et al., Phys. Rev. Lett. 82, 711 (1999)

$$\Delta E = 4\,463\,302(4)\,\mathrm{kHz}$$

S.Kanda et al. (MuSEUM), Phys. Lett. B 815, 136154 (2021)

The new work has an uncertainty goal of ±5 Hz P.Strasser et. al. (MuSEUM) EPJ Web of Conferences 198, 00003 (2019)

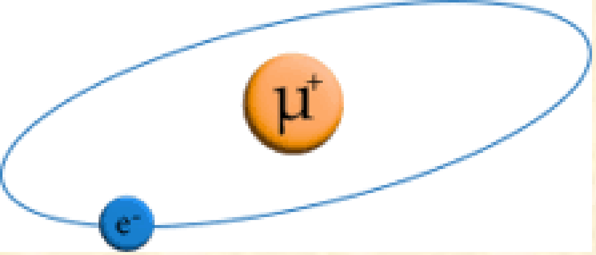

psas_2026

Muonium Spectrum

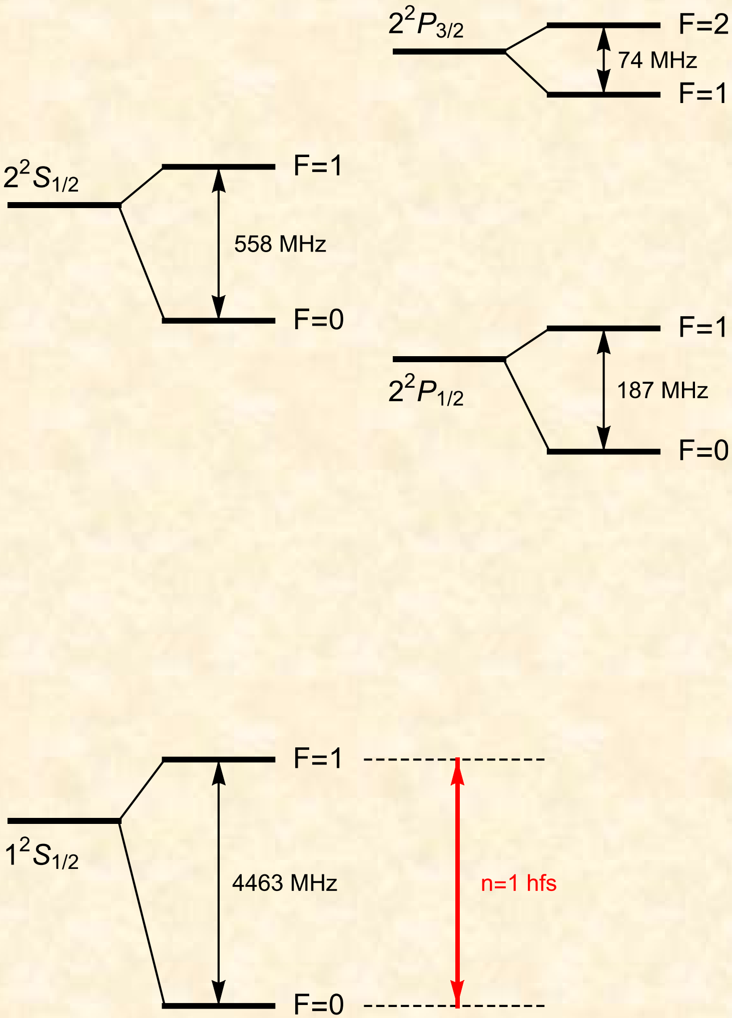

The n=1 hyperfine interval has been measured to high precision:

$$\Delta E = 4\,463\,302.88(16)\,\mathrm{kHz} \qquad \text{(Marion 1982)}$$

$$\Delta E = 4\,463\,302.765(53)\,\mathrm{kHz} \qquad \text{(Liu 1999)}$$

$$\Delta E = 4\,463\,302(4)\,\mathrm{kHz} \qquad \text{(Kanda 2021)}$$

The new experimental work has an uncertainty goal of ±5 Hz.

Theoretical prediction:

$$\Delta E = 4\,463\,302.868(271)\,\mathrm{kHz}$$

Mohr, Newell, Taylor, Rev. Mod. Phys. 88, 035009 (2016)

$$\Delta E = 4\,463\,302.872(515)\,\mathrm{kHz}$$

Eides, Phys. Lett. B 795, 113 (2019)

See also Karshenboim and Korzinin, Phys. Rev. A 103, 022805 (2021)

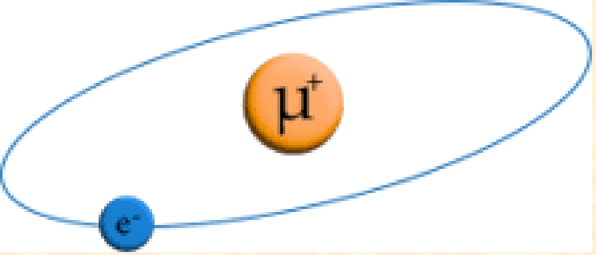

Muonium Spectrum

psas_2026

$$\tilde{E}_F = \frac{8m_e\alpha^4}{3}\left(\frac{m_r}{m_e}\right)^3\left(\frac{m_e}{m_\mu}\right) = 4454\,\mathrm{MHz}$$

$$\alpha^2\tilde{E}_F\left(\frac{m_e}{m_\mu}\right) = 1147\,\mathrm{Hz}\,,$$

$$\alpha^2\tilde{E}_F\left(\frac{m_e}{m_\mu}\right)^2 = 5.5\,\mathrm{Hz}\,,$$

$$\alpha^3\tilde{E}_F\left(\frac{m_e}{m_\mu}\right) = 8.4\,\mathrm{Hz}$$

$$\ln\left(\frac{1}{\alpha}\right) = 4.92\ ,\ \ln\left(\frac{m_\mu}{m_e}\right) = 5.33$$

The n=1 hyperfine interval has been measured to high precision:

$$\Delta E = 4\,463\,302.88(16)\,\mathrm{kHz}$$

$$\Delta E = 4\,463\,302.765(53)\,\mathrm{kHz}$$

$$\Delta E = 4\,463\,302(4)\,\mathrm{kHz}$$

The new experimental work has an uncertainty goal of ±5 Hz.

Theoretical prediction:

$\Delta E = 4\,463\,302.868(271)\,\mathrm{kHz}$

Mohr, Newell, Taylor, Rev. Mod. Phys. 88, 035009 (2016). [th: ±85 Hz]

$\Delta E = 4\,463\,302.872(515)\,\mathrm{kHz}$ [th: ±70 Hz]

Eides, Phys. Lett. B 795, 113 (2019)

See also Karshenboim and Korzinin, Phys. Rev. A 103, 022805 (2021)

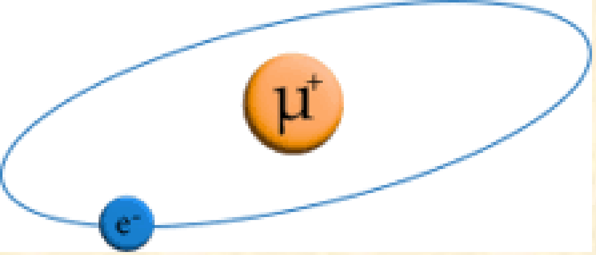

psas_2026

Muonium Spectrum

$$\tilde{E}_F = \frac{8 m_e \alpha^4}{3} \left(\frac{m_r}{m_e}\right)^3 \left(\frac{m_e}{m_\mu}\right) = 4454\,\mathrm{MHz}$$

$$\alpha^2 \tilde{E}_F \left(\frac{m_e}{m_\mu}\right) = 1147\,\mathrm{Hz}\,,$$

$$\alpha^2 \tilde{E}_F \left(\frac{m_e}{m_\mu}\right)^2 = 5.5\,\mathrm{Hz}\,,$$

$$\alpha^3 \tilde{E}_F \left(\frac{m_e}{m_\mu}\right) = 8.4\,\mathrm{Hz}$$

$$\ln\left(\frac{1}{\alpha}\right) = 4.92 \quad , \quad \ln\left(\frac{m_\mu}{m_e}\right) = 5.33$$

The n=1 hyperfine interval has been measured to high precision:

$$\Delta E = 4\,463\,302.88(16)\,\mathrm{kHz}$$

$$\Delta E = 4\,463\,302.765(53)\,\mathrm{kHz}$$

$$\Delta E = 4\,463\,302(4)\,\mathrm{kHz}$$

The new experimental work has an uncertainty goal of ±5 Hz.

Theoretical prediction:

$$\Delta E = 4\,463\,302.868(271)\,\mathrm{kHz}$$

Mohr, Newell, Taylor, Rev. Mod. Phys. 88, 035009 (2016). [th: ±85 Hz]

$$\Delta E = 4\,463\,302.872(515)\,\mathrm{kHz}$$ [th: ±70 Hz]

Eides, Phys. Lett. B 795, 113 (2019)

See also Karshenboim and Korzinin, Phys. Rev. A 103, 022805 (2021)

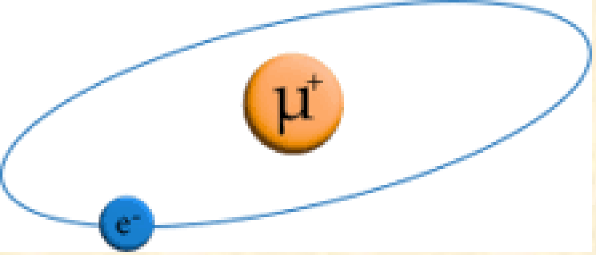

Method of Calculation

1. Use Non-Relativistic QED (NRQED) and dimensional regularization
2. Obtain all required matching coefficients. (Finding the contact term matching coefficients is an essential part of the recoil calculation, and is a significant challenge.)
3. Describe two-body bound states using the NRQED Bethe-Salpeter equation. Energies appear as poles in the Green function
4. Build a perturbation scheme based on an exact lowest-order solution to the NRQED Bethe-Salpeter equation
5. Use "expansion by regions" to identify contributions at various powers of the expansion parameter α
6. Express all contributions in terms of expectation values of various operators in states of the D-dimensional non-relativistic Schrödinger- Coulomb equation. Take the limit $D = 3\text{-}2\epsilon \rightarrow 3$

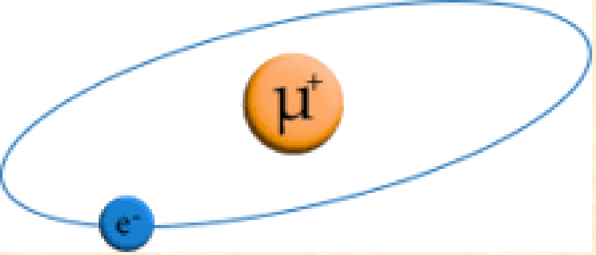

Method of Calculation

psas_2026

1. Use Non-Relativistic QED (NRQED) and dimensional regularization
2. Obtain all required matching coefficients. (Finding the contact term matching coefficients is an essential part of the recoil calculation, and is a significant challenge.)
3. Describe two-body bound states using the NRQED Bethe-Salpeter equation. Energies appear as poles in the Green function
4. Build a perturbation scheme based on an exact lowest-order solution to the NRQED Bethe-Salpeter equation
5. Use "expansion by regions" to identify contributions at various powers of the expansion parameter α
6. Express all contributions in terms of expectation values of various operators in states of the D-dimensional non-relativistic Schrödinger- Coulomb equation. Take the limit $D = 3\text{-}2\epsilon \rightarrow 3$

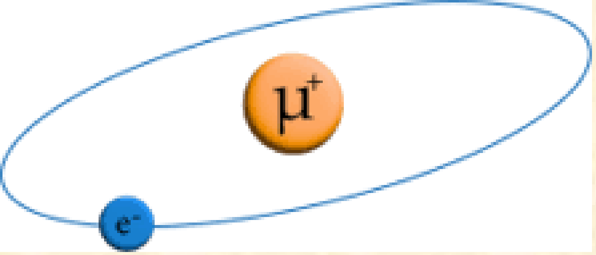

psas_2026

NRQED Feynman Rules

Interaction Vertices:

Coulomb

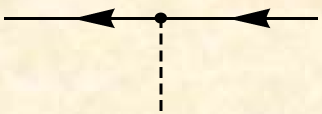

$-\mathrm{i}q$

Spin–Orbit

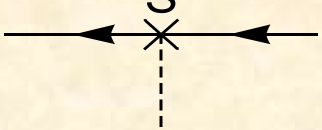

$c_S \dfrac{q}{4\,m^2}(\vec{p}_2\times\vec{p}_1)\cdot\vec{\sigma}$

Convection

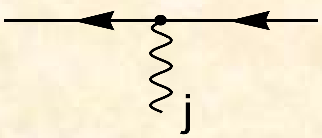

$\dfrac{\mathrm{i}q}{2\,m}(p_2+p_1)_j$

Darwin

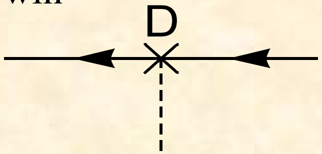

$c_D \dfrac{\mathrm{i}q}{8\,m^2}(\vec{p}_2-\vec{p}_1)^2$

Fermi

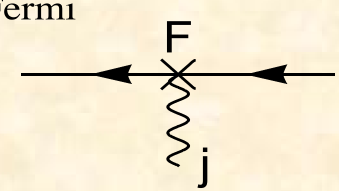

$c_F \dfrac{q}{2\,m}[(\vec{p}_2-\vec{p}_1)\times\vec{\sigma}]_j$

Seagull

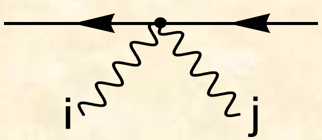

$\dfrac{-\mathrm{i}q^2}{m}\delta_{\mathrm{ij}}$

Contact

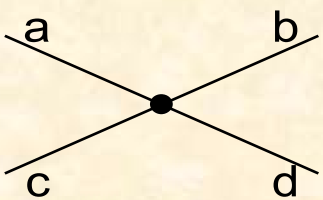

$\dfrac{d_s}{m^2}\delta_{\mathrm{ab}}\delta_{\mathrm{cd}} + \dfrac{d_v}{m^2}\vec{\sigma}_{\mathrm{ab}}\cdot\vec{\sigma}_{\mathrm{cd}}$

$+\cdots$

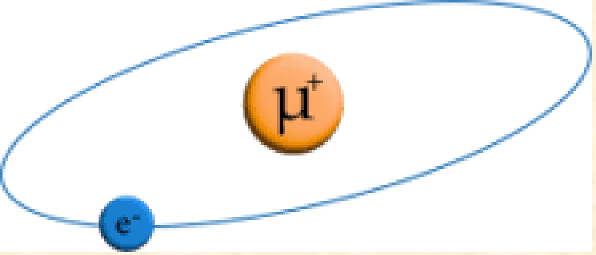

NRQED Feynman Rules

Interaction Vertices:

Coulomb

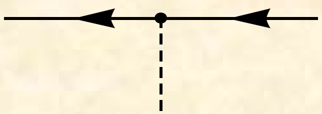

$$-iq$$

Spin–Orbit

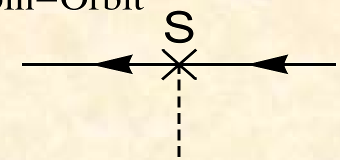

$$c_S \frac{q}{4\,m^2}(\vec{p}_2 \times \vec{p}_1)\cdot\vec{\sigma}$$

Convection

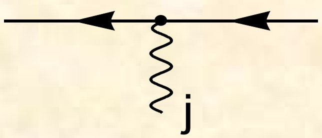

$$\frac{iq}{2\,m}(p_2+p_1)_j$$

Darwin

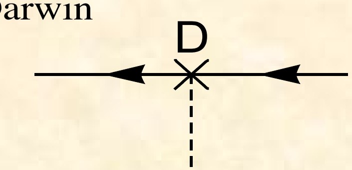

$$c_D \frac{iq}{8\,m^2}(\vec{p}_2-\vec{p}_1)^2$$

Fermi

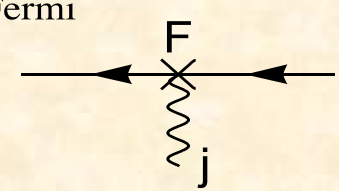

$$c_F \frac{q}{2\,m}[(\vec{p}_2-\vec{p}_1)\times\vec{\sigma}]_j$$

Seagull

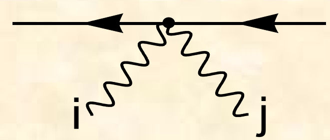

$$\frac{-iq^2}{m}\delta_{ij}$$

Contact

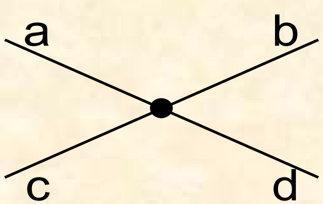

$$\frac{d_s}{m^2}\delta_{ab}\delta_{cd} + \frac{d_v}{m^2}\vec{\sigma}_{ab}\cdot\vec{\sigma}_{cd}$$

$$+\cdots$$

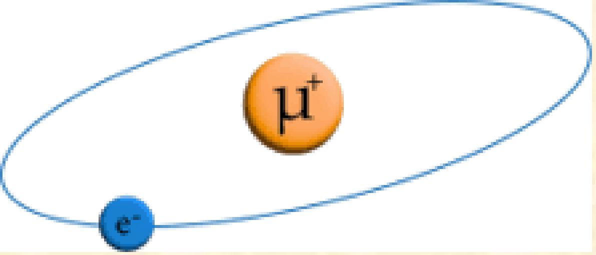

The NRQED Contact Term

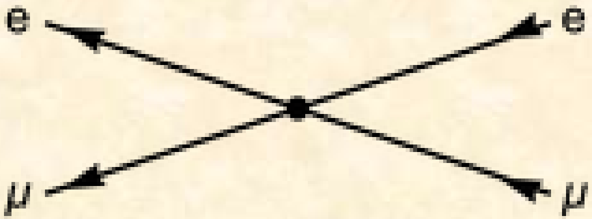

The NRQED contact term contains the contributions of all photon-exchange diagrams (possibly including radiative corrections) containing purely relativistic momenta.

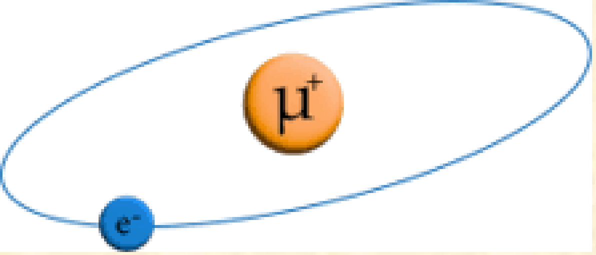

The NRQED Contact Term

The idea is that the space-time size of a relativistic process is small on an atomic scale.

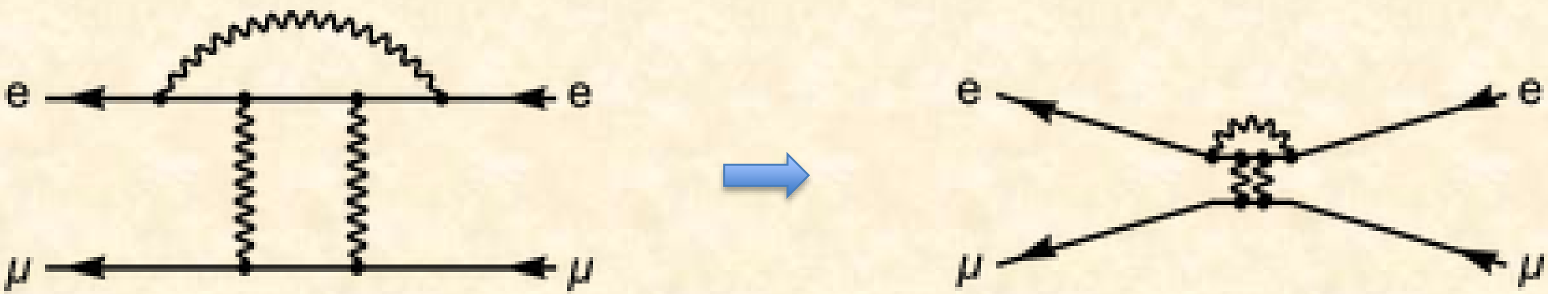

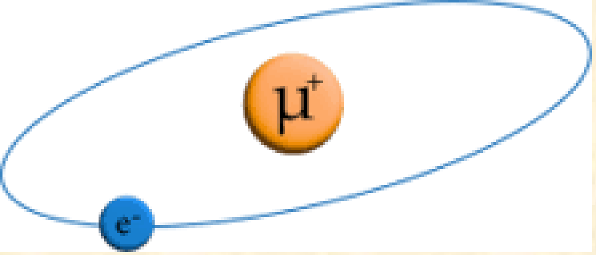

The NRQED Contact Term

The idea is that the space-time size of a relativistic process is small on an atomic scale.

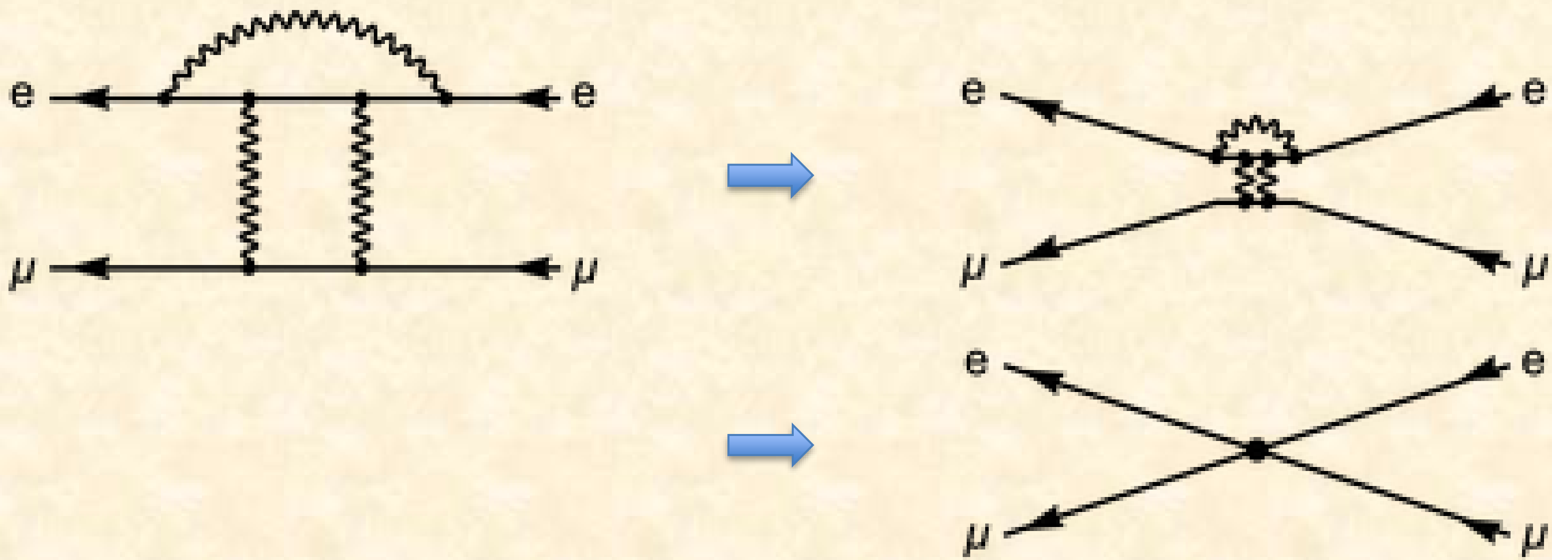

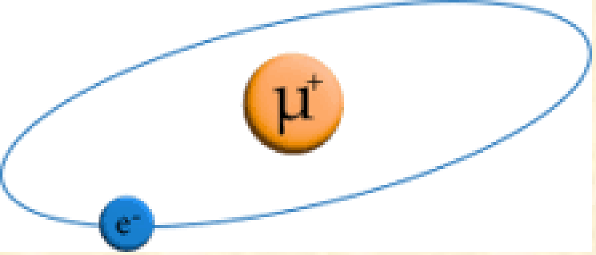

Energy Correction due to the Contact Term

The contact term contributes to an energy shift in NRQED by first order perturbation theory. The contact term matching coefficients are calculated from QED by taking the threshold limit of graphs where all loop momenta are hard (*i.e.* relativistic). Because the contact term has all particles meeting at a point, the energy shift is proportional to the square of the wave function at contact (*i.e.* at zero relative displacement).

$\Delta E \propto$ 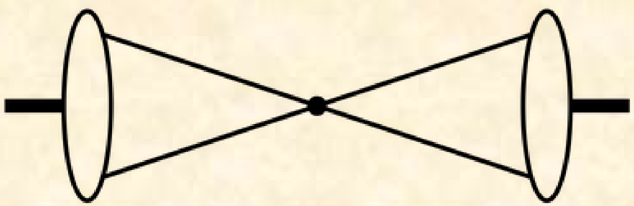 $\propto \ |\psi(0)|^2$ 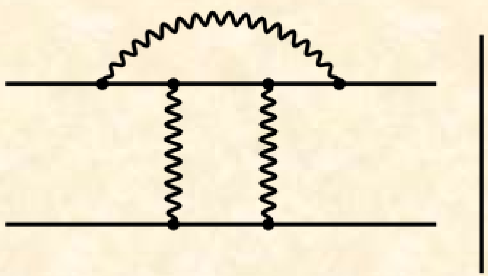 threshold

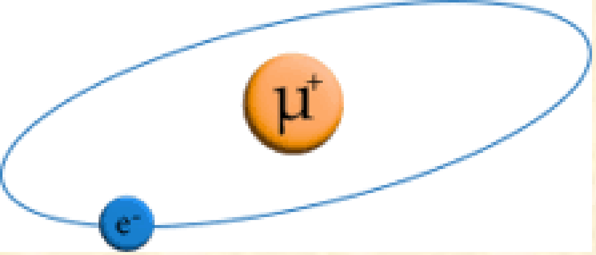

Energy Correction due to the Contact Term

The contact term contributes to an energy shift in NRQED by first order perturbation theory. The contact term matching coefficients are calculated from QED by taking the threshold limit of graphs where all loop momenta are hard (*i.e.* relativistic). Because the contact term has all particles meeting at a point, the energy shift is proportional to the square of the wave function at contact (*i.e.* at zero relative displacement).

$\Delta E \propto$ 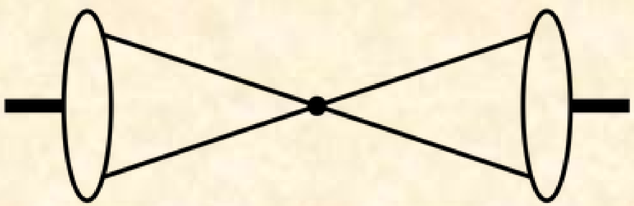 $\propto \; |\psi(0)|^2$ 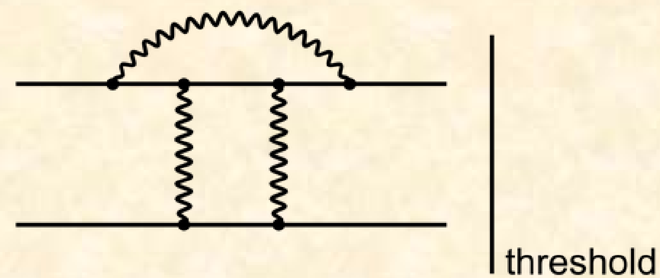

$$\Delta E = -|\psi(0)|^2 \mathcal{M} = -\frac{m_r^3 (Z\alpha)^3}{\pi n^3} \mathcal{M}$$

where $\mathcal{M}$ is the amplitude for hard corrections to QED threshold scattering

Radiative – Recoil Diagrams at Order $\alpha(Z\alpha)^5$

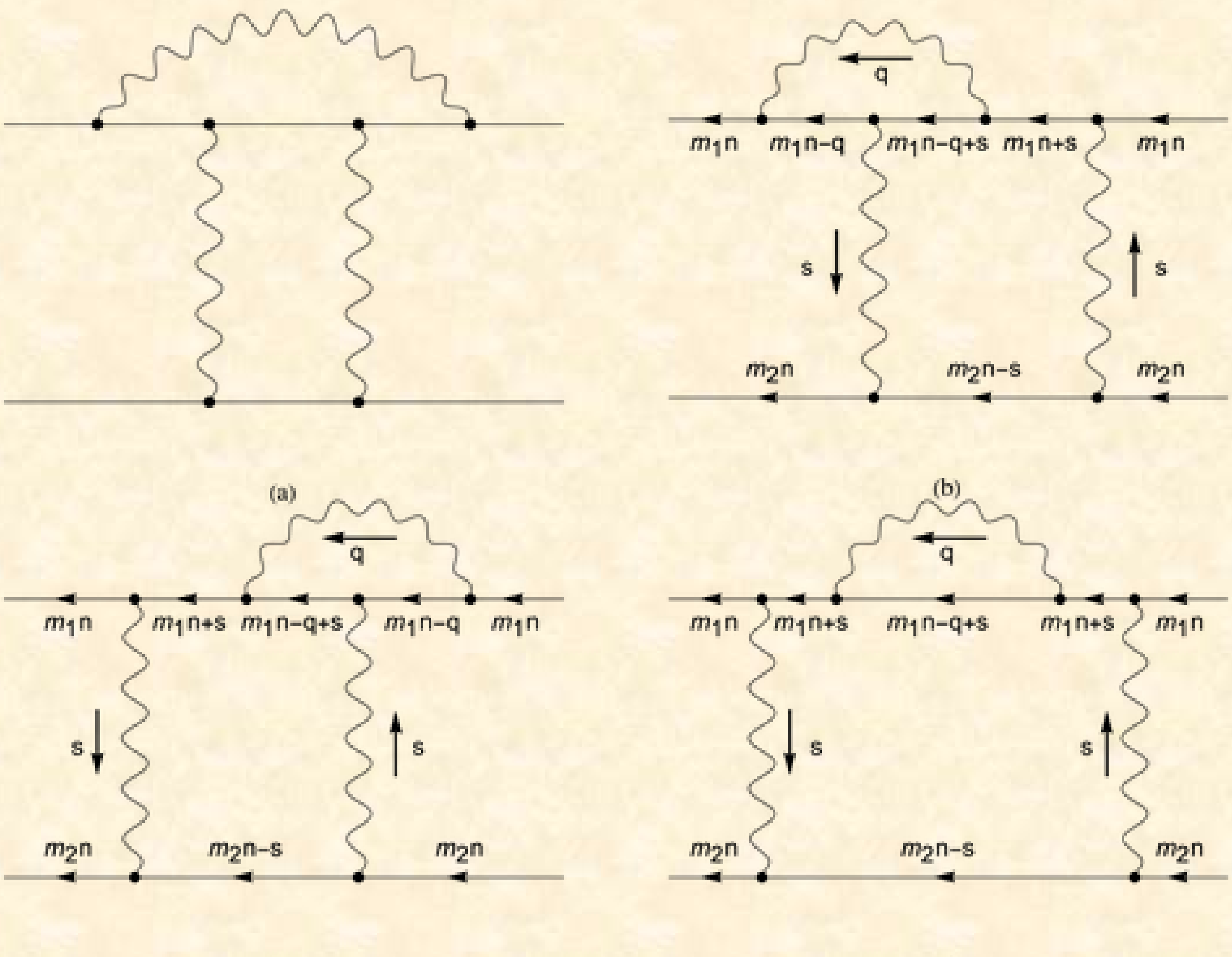

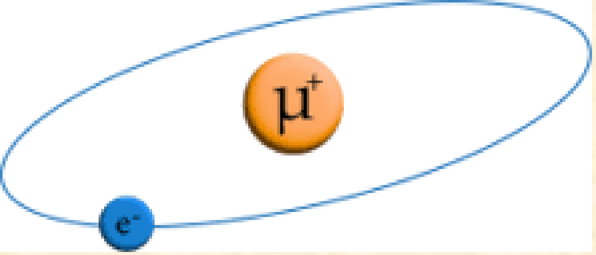

psas_2026

Radiative-Recoil Correction to Muonium hfs

$$\Delta E_{\rm hfs} = \left\{ \frac{8(Z\alpha)^4 m_r^3}{3 m_1 m_2} \right\} \frac{\alpha(Z\alpha)}{n^3} R_{\rm hfs} \qquad m_r = \frac{m_1 m_2}{m_1 + m_2} \quad , \quad x = \frac{m_1}{m_2}$$

$$\begin{aligned}
R_{\rm hfs}(x) \;=\; & \frac{1}{24\pi^2 x (1-x^2)^2} \Big\{ \pi^2 x \left(-78 + 14x + 159x^2 - 2x^3 - 99x^4 + 6x^5\right) \\
& + 36x^2 \left(4 - 5x^2 + x^4\right) \zeta(3) + 24\pi^2 x \left(1 + 3x - 8x^2 - 3x^3 + 7x^4\right) \log(2) \\
& + 24x^2 \left(-1 + x^2\right) \log(x) + 12 \left(x^2 - x^4 + 3x^6\right) \log^2(x) \\
& + 6(1-x)^2 \left(3 - 5x - 33x^2 - 19x^3 + 6x^4\right) \mathrm{HPL}(\{1,0\},x) \\
& - 6(1+x)^2 \left(3 + 5x - 33x^2 + 19x^3 + 6x^4\right) \mathrm{HPL}(\{-1,0\},x) \\
& + x(1+x)^2 \left(1 - 9x + 9x^2 - x^3\right) \Big[2\pi^2 \mathrm{HPL}(\{1\},x) + 12\,\mathrm{HPL}(\{-2,0\},x) \\
& \qquad - 12\,\mathrm{HPL}(\{1,0,0\},x) + 24\,\mathrm{HPL}(\{1,-1,0\},x) \Big] \\
& + x(1-x)^2 \left(1 + 9x + 9x^2 + x^3\right) \Big[-4\pi^2 \mathrm{HPL}(\{-1\},x) + 12\,\mathrm{HPL}(\{2,0\},x) \\
& \qquad - 12\,\mathrm{HPL}(\{-1,0,0\},x) - 24\,\mathrm{HPL}(\{-1,1,0\},x) \Big] \Big\}
\end{aligned}$$

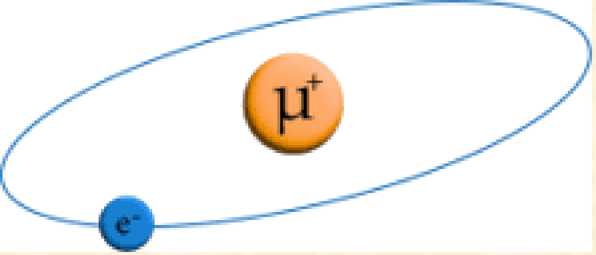

Radiative-Recoil Correction to Muonium hfs

$$\Delta E_{\rm hfs} = \left\{ \frac{8(Z\alpha)^4 m_r^3}{3 m_1 m_2} \right\} \frac{\alpha (Z\alpha)}{n^3} R_{\rm hfs} \qquad m_r = \frac{m_1 m_2}{m_1 + m_2} \quad , \quad x = \frac{m_1}{m_2}$$

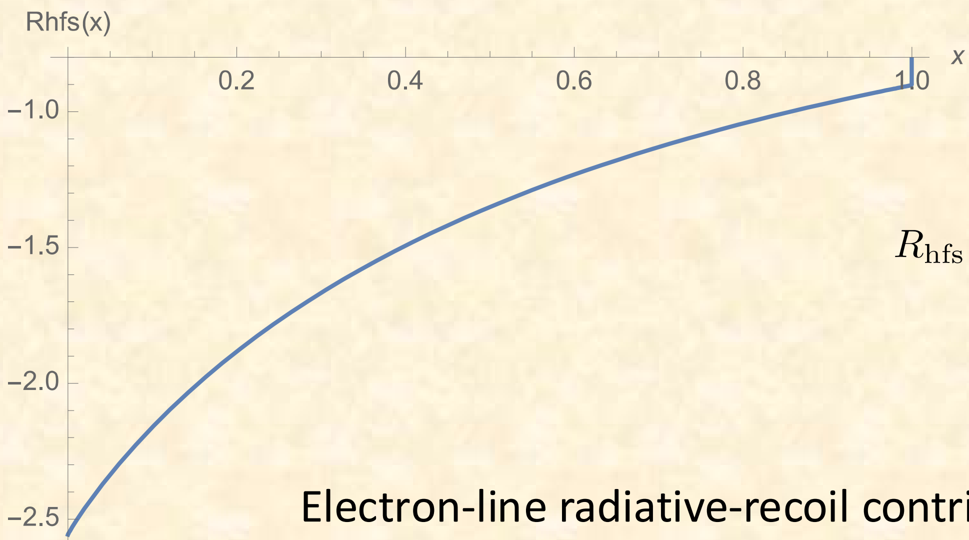

Positronium limiting case:

$$R_{\rm hfs}(1) = \frac{1}{\pi^2} \left\{ \frac{3}{4}\zeta(3) + 2\pi^2 \ln 2 - \frac{79\pi^2}{32} + \frac{7}{8} \right\}$$

Electron-line radiative-recoil contribution for muonium:

$$R_{\rm hfs}(x) = \left(-\frac{13}{4} + \ln 2 \right) + \frac{x}{\pi^2} \left(-\frac{15}{4} \ln x + 6\zeta(3) + 3\pi^2 \ln 2 + \frac{\pi^2}{2} + \frac{17}{8} \right) + x^2 \left(-\frac{3}{2} - 6 \ln 2 \right) + O(x^3)$$

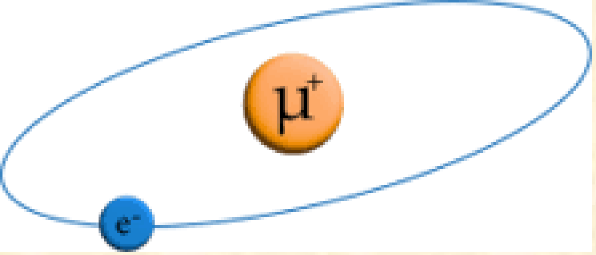

Radiative-Recoil Correction to Muonium hfs

$$\Delta E_{\mathrm{hfs}} = \left\{ \frac{8(Z\alpha)^4 m_r^3}{3 m_1 m_2} \right\} \frac{\alpha (Z\alpha)}{n^3} R_{\mathrm{hfs}} \qquad m_r = \frac{m_1 m_2}{m_1 + m_2} \quad , \quad x = \frac{m_1}{m_2}$$

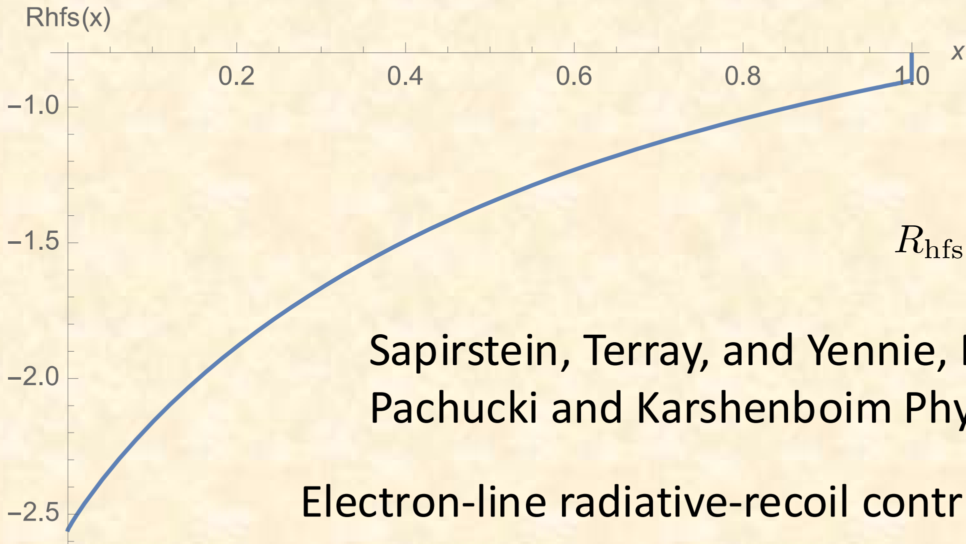

Positronium limiting case:

$$R_{\mathrm{hfs}}(1) = \frac{1}{\pi^2} \left\{ \frac{3}{4}\zeta(3) + 2\pi^2 \ln 2 - \frac{79\pi^2}{32} + \frac{7}{8} \right\}$$

Sapirstein, Terray, and Yennie, Phys. Rev. D 29, 2290 (1984) – numerical

Pachucki and Karshenboim Phys. Rev. Lett. 80, 2101 (1998) – analytical

Electron-line radiative-recoil contribution for muonium:

$$R_{\mathrm{hfs}}(x) = \left(-\frac{13}{4} + \ln 2 \right) + \frac{x}{\pi^2} \left(-\frac{15}{4} \ln x + 6\zeta(3) + 3\pi^2 \ln 2 + \frac{\pi^2}{2} + \frac{17}{8} \right) + x^2 \left(-\frac{3}{2} - 6 \ln 2 \right) + O(x^3)$$

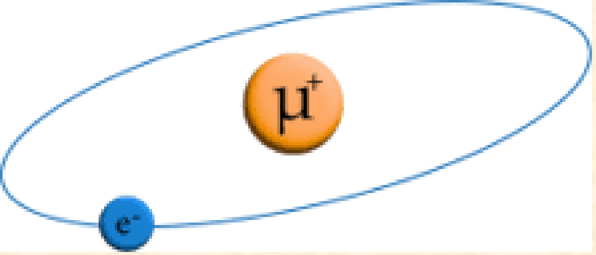

psas_2026

Radiative-Recoil Correction to Muonium hfs

$$\Delta E_{\rm hfs} = \left\{ \frac{8(Z\alpha)^4 m_r^3}{3 m_1 m_2} \right\} \frac{\alpha(Z\alpha)}{n^3} R_{\rm hfs} \qquad m_r = \frac{m_1 m_2}{m_1 + m_2} \quad , \quad x = \frac{m_1}{m_2}$$

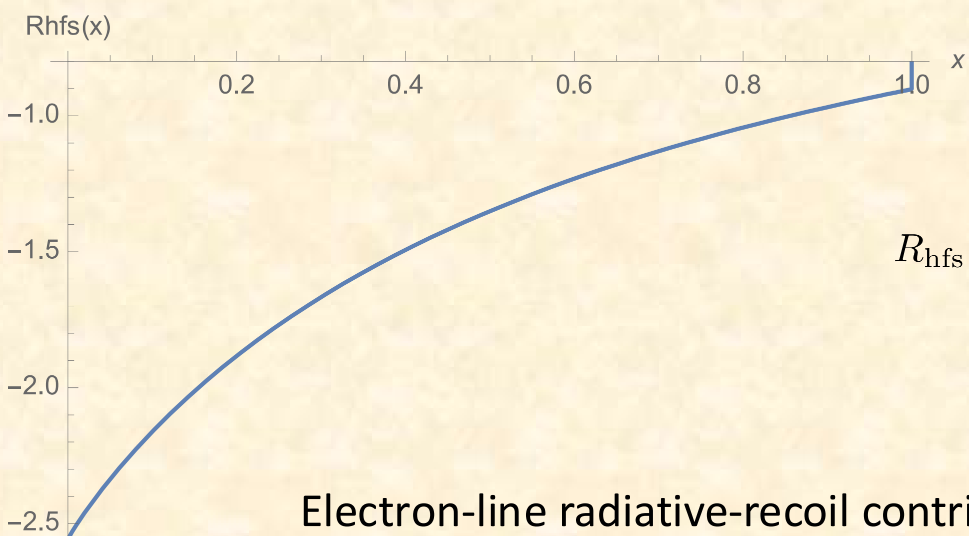

Positronium limiting case:

$$R_{\rm hfs}(1) = \frac{1}{\pi^2} \left\{ \frac{3}{4}\zeta(3) + 2\pi^2 \ln 2 - \frac{79\pi^2}{32} + \frac{7}{8} \right\}$$

Electron-line radiative-recoil contribution for muonium:

$$R_{\rm hfs}(x) = \left(-\frac{13}{4} + \ln 2 \right) + \frac{x}{\pi^2} \left(-\frac{15}{4} \ln x + 6\zeta(3) + 3\pi^2 \ln 2 + \frac{\pi^2}{2} + \frac{17}{8} \right) + x^2 \left(-\frac{3}{2} - 6 \ln 2 \right) + O(x^3)$$

Terray and Yennie, Phys. Rev. Lett. 48, 1803 (1982)

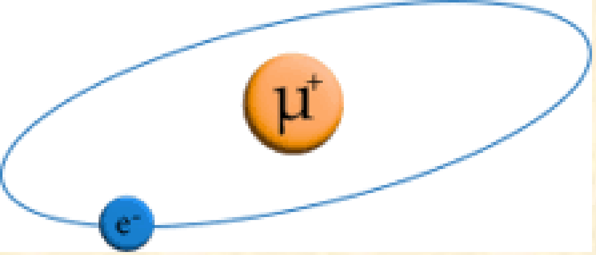

psas_2026

Radiative-Recoil Correction to Muonium hfs

$$\Delta E_{\text{hfs}} = \left\{ \frac{8(Z\alpha)^4 m_r^3}{3 m_1 m_2} \right\} \frac{\alpha(Z\alpha)}{n^3} R_{\text{hfs}} \qquad m_r = \frac{m_1 m_2}{m_1 + m_2} \quad , \quad x = \frac{m_1}{m_2}$$

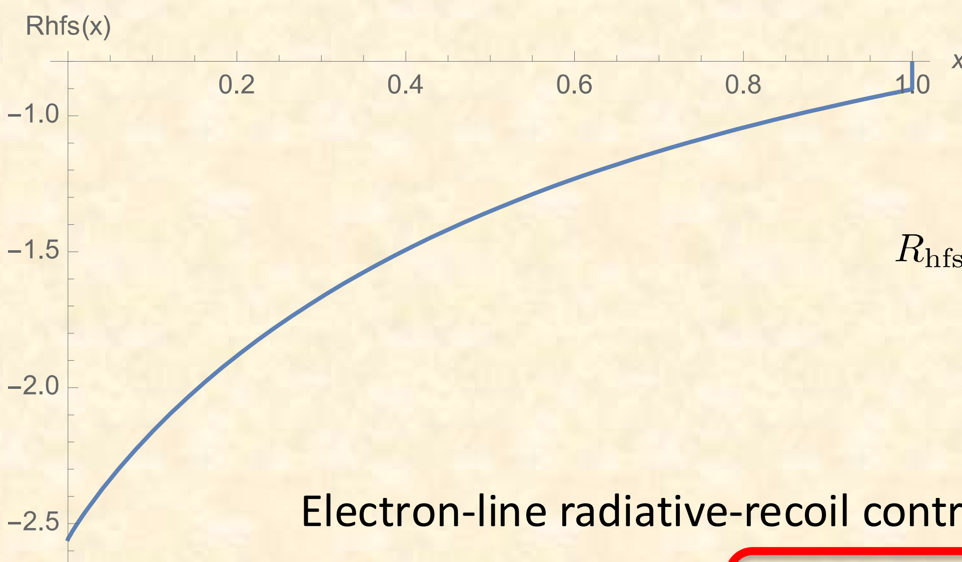

Positronium limiting case:

$$R_{\text{hfs}}(1) = \frac{1}{\pi^2} \left\{ \frac{3}{4}\zeta(3) + 2\pi^2 \ln 2 - \frac{79\pi^2}{32} + \frac{7}{8} \right\}$$

Electron-line radiative-recoil contribution for muonium:

$$R_{\text{hfs}}(x) = \left(-\frac{13}{4} + \ln 2 \right) + \frac{x}{\pi^2} \left(-\frac{15}{4} \ln x + 6\zeta(3) + 3\pi^2 \ln 2 + \frac{\pi^2}{2} + \frac{17}{8} \right) + x^2 \left(-\frac{3}{2} - 6 \ln 2 \right) + O(x^3)$$

Sapirstein, Terray, and Yennie, Phys. Rev. Lett. 48, 1803 (1982) – numerical
Eides, Karshenboim, and Shelyuto, Phys. Lett. B 177, 425 (1986) – analytical

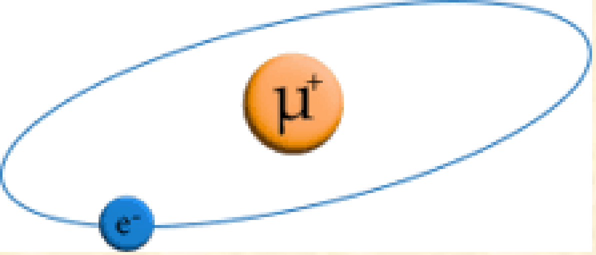

psas_2026

Radiative-Recoil Correction to Muonium hfs

$$\Delta E_{\text{hfs}} = \left\{\frac{8(Z\alpha)^4 m_r^3}{3m_1 m_2}\right\}\frac{\alpha(Z\alpha)}{n^3}R_{\text{hfs}} \qquad m_r = \frac{m_1 m_2}{m_1+m_2} \quad , \quad x = \frac{m_1}{m_2}$$

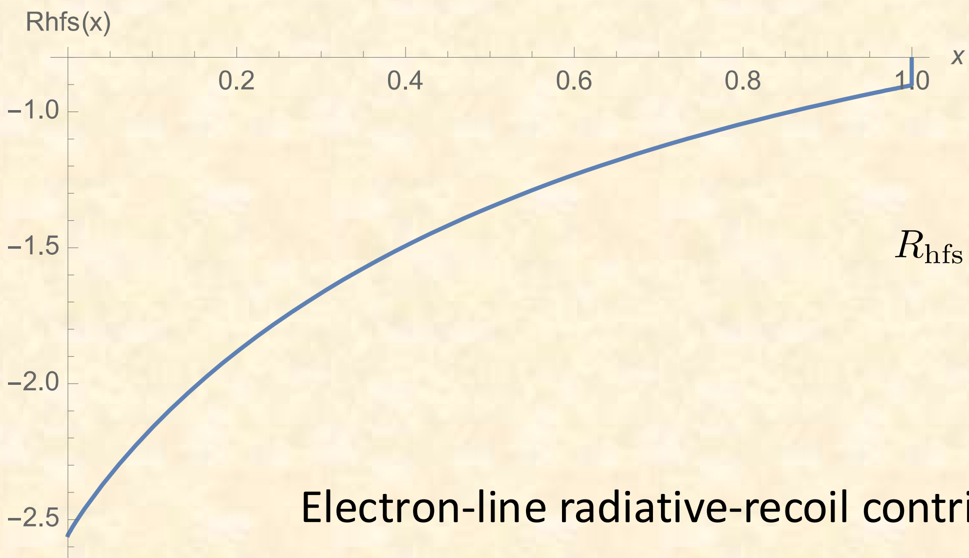

Positronium limiting case:

$$R_{\text{hfs}}(1) = \frac{1}{\pi^2}\left\{\frac{3}{4}\zeta(3) + 2\pi^2\ln 2 - \frac{79\pi^2}{32} + \frac{7}{8}\right\}$$

Electron-line radiative-recoil contribution for muonium:

$$R_{\text{hfs}}(x) = \left(-\frac{13}{4} + \ln 2\right) + \frac{x}{\pi^2}\left(-\frac{15}{4}\ln x + 6\zeta(3) + 3\pi^2\ln 2 + \frac{\pi^2}{2} + \frac{17}{8}\right) + x^2\left(-\frac{3}{2} - 6\ln 2\right) + O(x^3)$$

Eides, Grotch, and Shelyuto, Phys. Rev. D 58,013008 (1998)

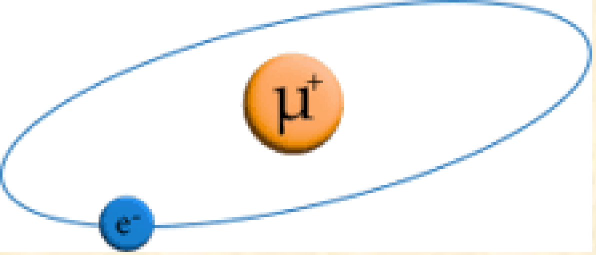

Radiative-Recoil Correction to Muonium hfs

$$\Delta E_{\text{hfs}} = \left\{ \frac{8(Z\alpha)^4 m_r^3}{3 m_1 m_2} \right\} \frac{\alpha (Z\alpha)}{n^3} R_{\text{hfs}} \qquad m_r = \frac{m_1 m_2}{m_1 + m_2} \quad , \quad x = \frac{m_1}{m_2}$$

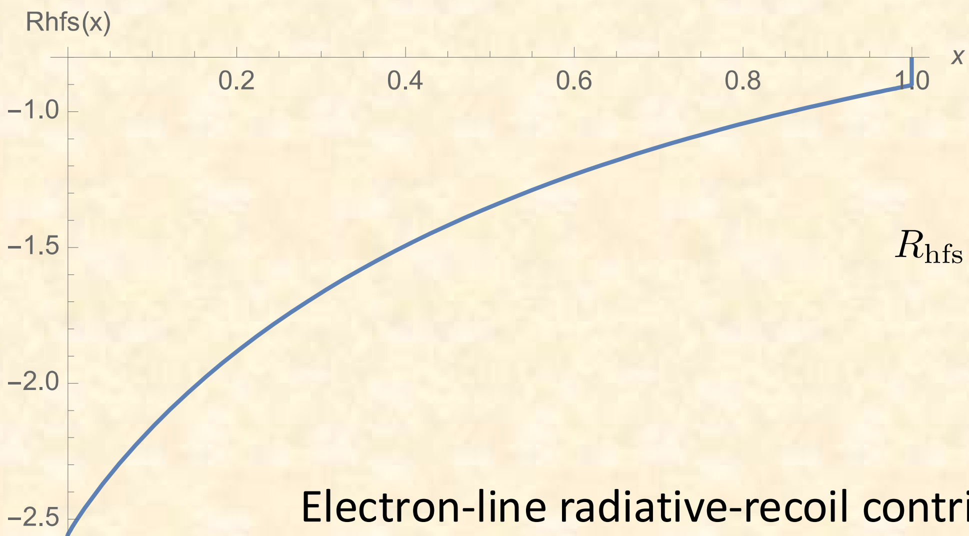

Positronium limiting case:

$$R_{\text{hfs}}(1) = \frac{1}{\pi^2} \left\{ \frac{3}{4}\zeta(3) + 2\pi^2 \ln 2 - \frac{79\pi^2}{32} + \frac{7}{8} \right\}$$

Electron-line radiative-recoil contribution for muonium:

$$R_{\text{hfs}}(x) = \left(-\frac{13}{4} + \ln 2 \right) + \frac{x}{\pi^2} \left(-\frac{15}{4} \ln x + 6\zeta(3) + 3\pi^2 \ln 2 + \frac{\pi^2}{2} + \frac{17}{8} \right) + x^2 \left(-\frac{3}{2} - 6 \ln 2 \right) + O(x^3)$$

Expansion out to $O(x^6)$: Blokland, Czarnecki, and Melnikov, Phys. Rev. D <u>65</u>,073015 (2002)

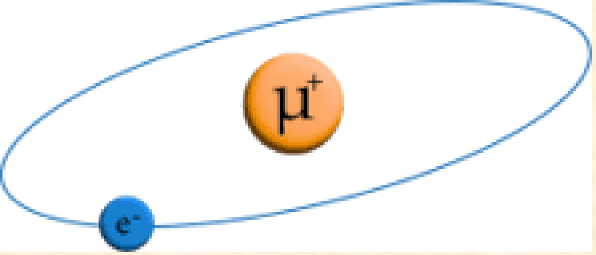

Next Steps: Recoil and Radiative-Recoil Corrections at order α^7

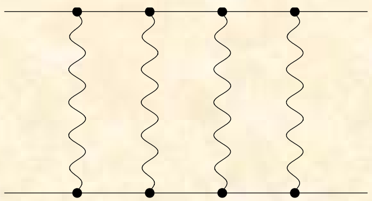

Pure recoil at order $$\frac{m_e(Z\alpha)^7}{n^3}\left(\frac{m_r}{m_e}\right)^3\left(\frac{m_e}{m_\mu}\right)$$

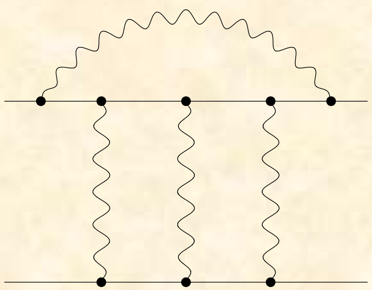

Radiative-recoil at order $$\frac{m_e\alpha(Z\alpha)^6}{n^3}\left(\frac{m_r}{m_e}\right)^3\left(\frac{m_e}{m_\mu}\right)$$

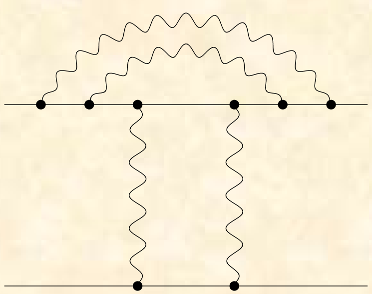

Radiative-recoil at order $$\frac{m_e\alpha^2(Z\alpha)^5}{n^3}\left(\frac{m_r}{m_e}\right)^3\left(\frac{m_e}{m_\mu}\right)$$

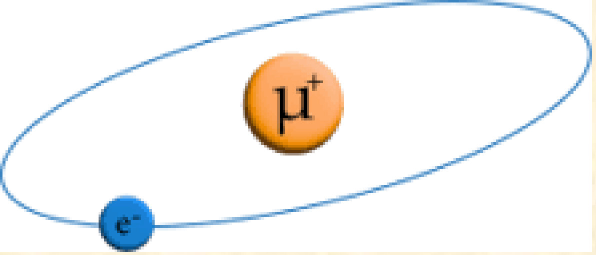

Next Steps:
Recoil and Radiative-Recoil Corrections at order α^7

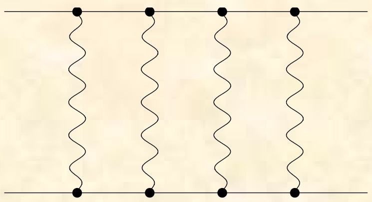

Pure recoil at order $$\frac{m_e(Z\alpha)^7}{n^3}\left(\frac{m_r}{m_e}\right)^3\left(\frac{m_e}{m_\mu}\right)$$

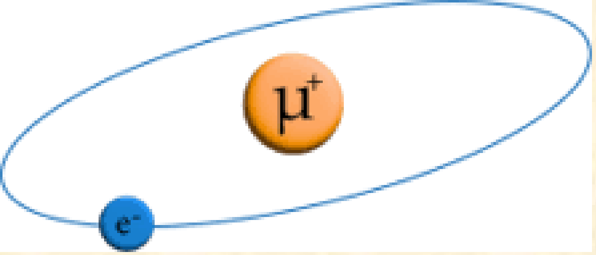

Next Steps: Recoil and Radiative-Recoil Corrections at order α^7

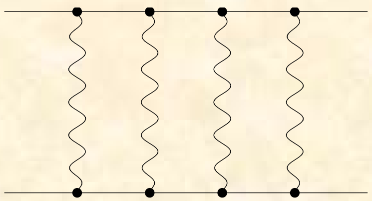

Pure recoil at order $$\frac{m_e(Z\alpha)^7}{n^3}\left(\frac{m_r}{m_e}\right)^3\left(\frac{m_e}{m_\mu}\right)$$

There are 4! = 24 permutations of the photon lines, giving diagrams with crossed photons. Of these, 18 are independent. After evaluating the numerator factors, there are 44290 Feynman integrals to evaluate. Integration by parts (IBP) identities were used to express these in terms of several hundred master integrals.

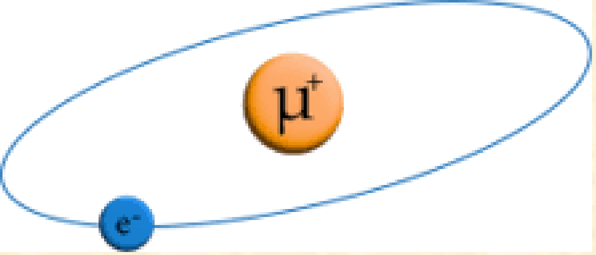

Next Steps: Recoil and Radiative-Recoil Corrections at order α^7

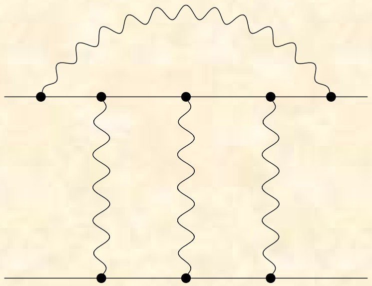

Radiative-recoil at order $$\frac{m_e\alpha(Z\alpha)^6}{n^3}\left(\frac{m_r}{m_e}\right)^3\left(\frac{m_e}{m_\mu}\right)$$

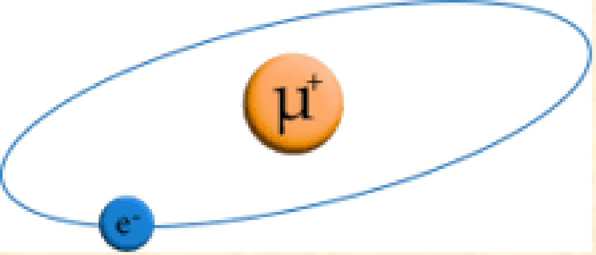

psas_2026

Next Steps: Recoil and Radiative-Recoil Corrections at order α^7

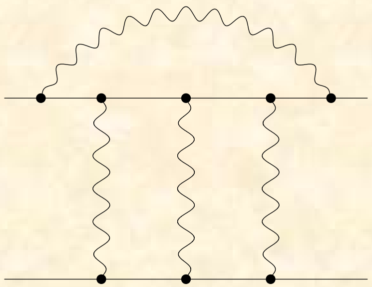

Radiative-recoil at order $$\frac{m_e \alpha (Z\alpha)^6}{n^3} \left(\frac{m_r}{m_e}\right)^3 \left(\frac{m_e}{m_\mu}\right)$$

There are 8 diagrams with ladder photons, and 3! = 6 permutations of those photons giving 6 x 8 = 48 diagrams when all diagrams with crossed photons are included. Of these, 26 are independent.

After evaluating the numerator factors, there were 31638 Feynman Integrals to do. The IBP relations were used to express these in terms of 277 master integrals.

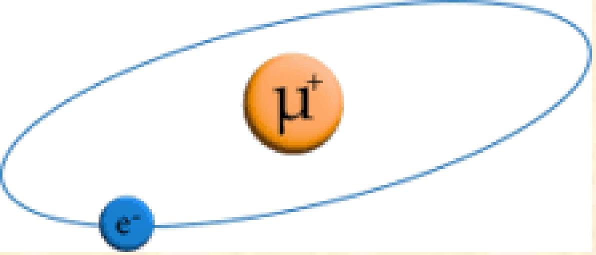

psas_2026

Next Steps: Recoil and Radiative-Recoil Corrections at order α^7

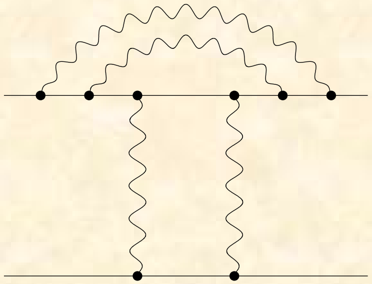

Radiative-recoil at order $$\frac{m_e\alpha^2(Z\alpha)^5}{n^3}\left(\frac{m_r}{m_e}\right)^3\left(\frac{m_e}{m_\mu}\right)$$

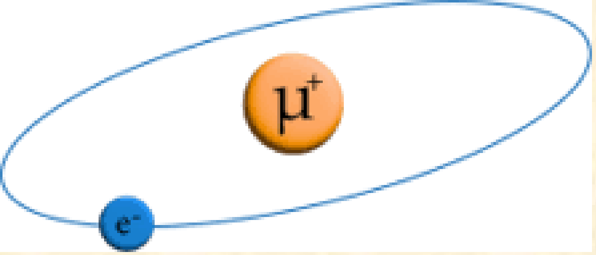

Radiative–Recoil Diagrams at Order $\alpha^2(Z\alpha)^5$

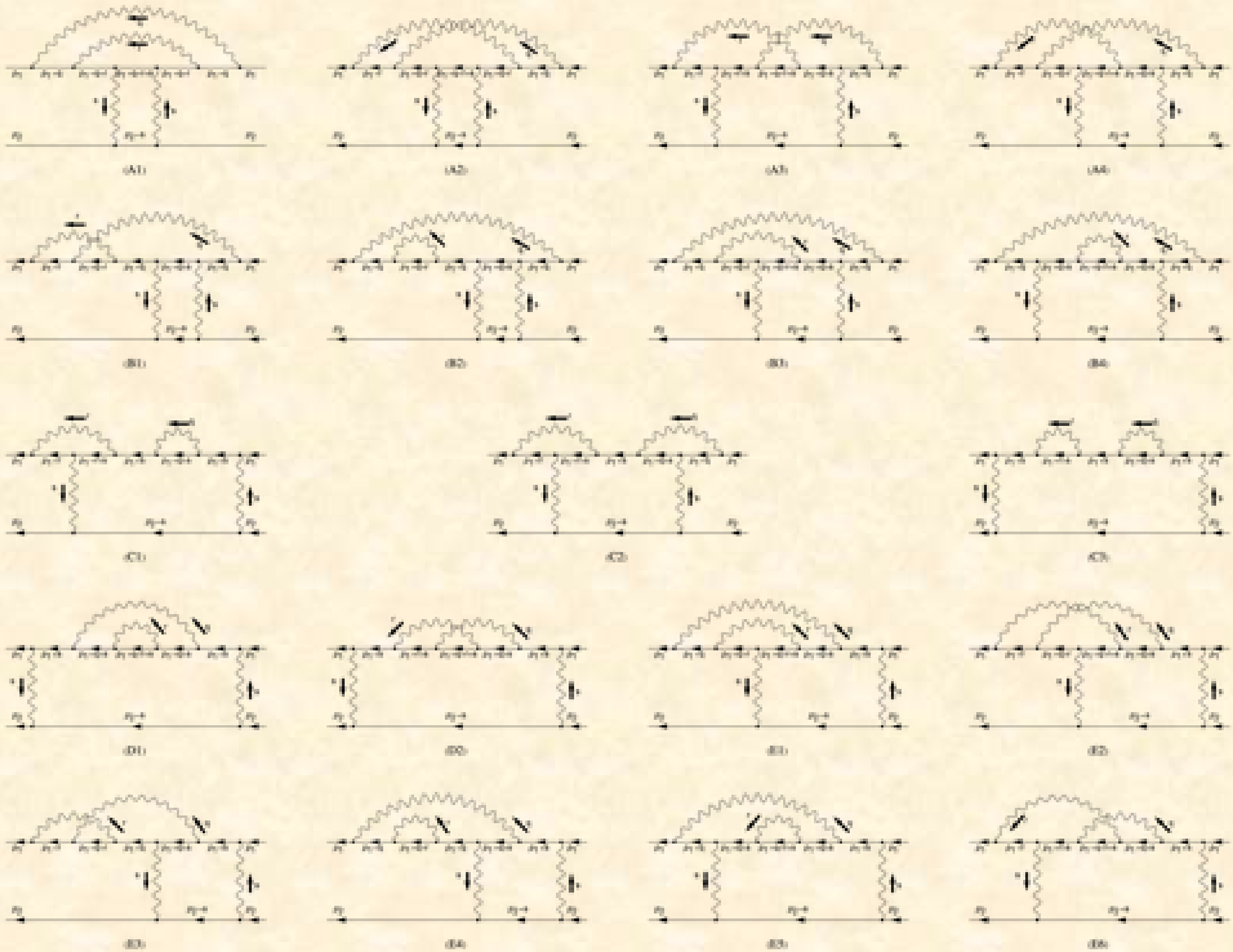

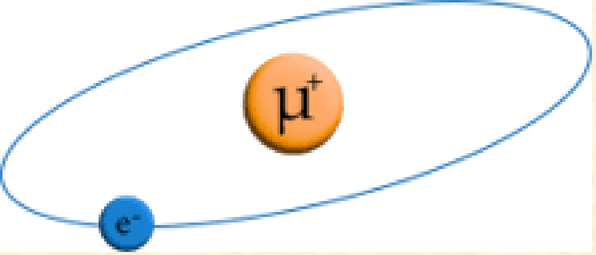

Radiative – Recoil Diagrams at Order $\alpha^2(Z\alpha)^5$

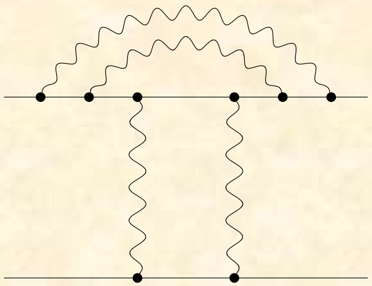

Radiative-recoil at order $$\frac{m_e\alpha^2(Z\alpha)^5}{n^3}\left(\frac{m_r}{m_e}\right)^3\left(\frac{m_e}{m_\mu}\right)$$

There are 19 diagrams with ladder photons, and two permutations of the photons (ladder and crossed) giving 2 x 19 = 38 diagrams when all diagrams with crossed photons are included. (Left-right symmetry has already been accounted for.) In all, there are 9155 separate three-loop Feynman integrals to compute.

The IBP relations have been used to express these 9155 integrals in terms of just 139 master integrals. The master integrals tend to be simpler than the ones they replace, but they are still non-trivial three-loop integrals.

Radiative – Recoil Diagrams at Order $\alpha^2(Z\alpha)^5$

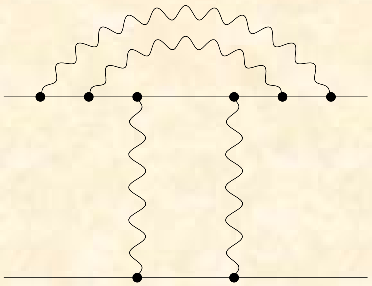

The electron-muon scattering amplitude (at threshold) due to these diagrams is the sum

$$\mathcal{M} = \sum_{k=1}^{139} A_k(x,\epsilon)\, I_k(x,\epsilon)\ ,$$

where $I_k(x,\epsilon)$ is the k^{th} master integral and $A_k(x,\epsilon)$ is its coefficient. Both the master integrals and their coefficients depend on the mass ratio *x* and the dimensional regularization factor ϵ.

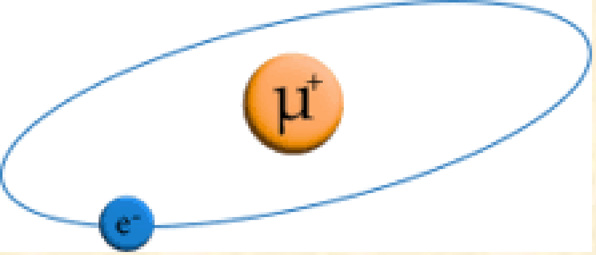

psas_2026

Radiative–Recoil Diagrams at Order $\alpha^2(Z\alpha)^5$

The master integrals involve anywhere from three to eight distinct fermion or photon denominators. The three-denominator integrals can be done analytically. The four-denominator integrals can be done analytically in terms of harmonic polynomials (which can be defined as a specific subset of iterated integrals) using the method of differential equations. Master integrals with yet more denominators typically involve more general functions than harmonic polynomials if they can be performed analytically at all. In our experience, five-denominator integrals require advanced techniques, and it seems impractical to attempt to find analytic expressions for most integrals with six or more denominators.

Radiative – Recoil Diagrams at Order $\alpha^2(Z\alpha)^5$

Typical three-denominator master integral:

$$I(3\text{–den}) = \Phi^3 \int \frac{d^dq}{(2\pi)^d}\frac{d^dr}{(2\pi)^d}\frac{d^ds}{(2\pi)^d}\Big[(-q^2+2xqn)(-s^2-2sn)$$

$$\times(-(q+r-s)^2+2x(q+r-s)n)\Big]^{-1}$$

$$= x^{4-4\epsilon}e^{3\epsilon\gamma_E}\,\Gamma^3(-1+\epsilon)$$

where $\Phi = -i(4\pi)^{2-\epsilon}e^{\epsilon\gamma_E}$

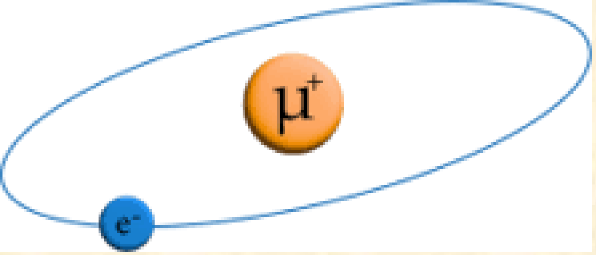

Radiative–Recoil Diagrams at Order $\alpha^2(Z\alpha)^5$

Typical four-denominator master integral:

$$
\begin{aligned}
I(4\text{–den}) &= \Phi^3 \int \frac{d^dq}{(2\pi)^d}\frac{d^dr}{(2\pi)^d}\frac{d^ds}{(2\pi)^d}\Big[(-r^2)(-q^2+2xqn)(-s^2-2sn) \\
&\qquad \times(-(q+r-s)^2+2x(q+r-s)n)\Big]^{-1} \\
&= \frac{1}{3\epsilon^3}x^2\left(x^2+2\right)+\frac{1}{\epsilon^2}\left\{\frac{1}{6}\left(7x^4+15x^2-1\right)-2\left(x^4+x^2\right)\ln x\right\} \\
&+ \frac{1}{\epsilon}\left\{\frac{1}{36}\Big[-35+3(71+2\pi^2)x^2+3(25+\pi^2)x^4)\Big]\right. \\
&\qquad \left. -7(x^2+x^4)\ln x+2(x^2+3x^4)\ln^2 x\right\} \\
&+ \left\{2(1-x^2)^2(1+x^2)\mathrm{HPL}[\{-1,0\},x]-8x^2(1-x^2)\mathrm{HPL}[\{0,1,0\},x]+\cdots\right\} \\
&+ \cdots
\end{aligned}
$$

The analytic result involves 601 distinct HPL functions having up to seven indices.

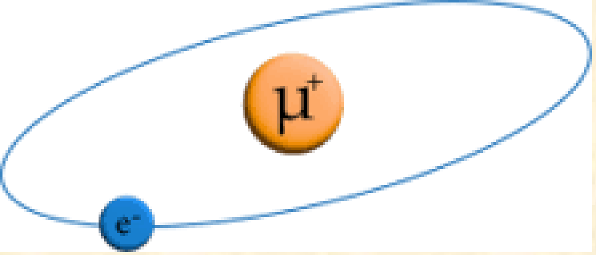

Radiative−Recoil Diagrams at Order $\alpha^2(Z\alpha)^5$

Typical eight-denominator master integral:

$$
\begin{aligned}
I(8-\text{den}) \quad = \quad \Phi^3 \int \frac{d^d q}{(2\pi)^d}\frac{d^d r}{(2\pi)^d}\frac{d^d s}{(2\pi)^d}\Big[&(-q^2)(-r^2)(-q^2+2xqn)(-r^2+2xrn) \\
&\times(-s^2-2sn)\big(-(q-s)^2+2x(q-s)n\big) \\
&\times\big(-(r-s)^2+2x(r-s)n\big)\big(-(q+r-s)^2+2x(q+r-s)n\big)\Big]^{-1}
\end{aligned}
$$

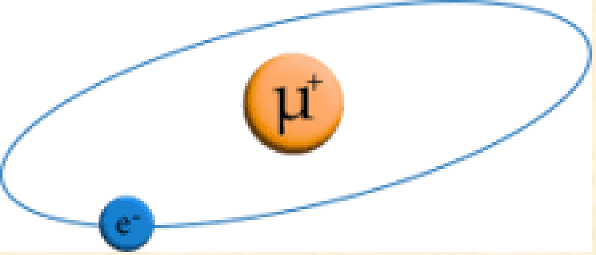

psas_2026

Radiative – Recoil Diagrams at Order $\alpha^2(Z\alpha)^5$

The coefficients are complicated functions of the mass ratio *x* and the dimensional regularization parameter ϵ. They can involve up to four inverse factors of ϵ, which implies that the corresponding master integrals must be evaluated through terms of order ϵ^4. So eight total orders in ϵ are required, from order $1/\epsilon^3$ through order ϵ^4.

The coefficients can also involve up to 13 inverse powers of the mass ratio *x*, which implies that the corresponding master integrals must be evaluated with high precision for *x* small (as in hydrogen and muonium). They also can involve high inverse powers of (1-*x*), which implies that the corresponding master integrals must be evaluated with high precision for *x* near 1 (as in positronium).

Radiative – Recoil Diagrams at Order $\alpha^2(Z\alpha)^5$

Plan 1: Evaluate the four-denominator and possibly the five-denominator integrals analytically. These are the ones whose coefficients have the highest inverse powers of *x*, *(1-x)*, and ϵ. Evaluate the six- through eight-denominator integrals numerically via sector decomposition followed by numerical integration, using either FIESTA or pySecDec, which handle the expansion in ϵ automatically. Problems: The analytical evaluations are time consuming and must be done individually. The numerical evaluation of the remaining integrals must be done one by one, and it might be difficult to achieve the needed precision for *x* near 0 or 1.

Radiative – Recoil Diagrams at Order $\alpha^2(Z\alpha)^5$

Plan 1: Evaluate the four-denominator and possibly the five-denominator integrals analytically. These are the ones whose coefficients have the highest inverse powers of *x*, *(1-x)*, and ϵ. Evaluate the six- through eight-denominator integrals numerically via sector decomposition followed by numerical integration, using either FIESTA or pySecDec, which handle the expansion in ϵ automatically. Problems: The analytical evaluations are time consuming and must be done individually. The numerical evaluation of the remaining integrals must be done one by one, and it might be difficult to achieve the needed precision for *x* near 0 or 1.

Plan 2: Evaluate all master integrals using the recently-developed “auxiliary mass flow” method. The package “AMFlow” evaluates all required integrals automatically. It handles the expansion in ϵ and allows numerical evaluation to arbitrarily high precision.

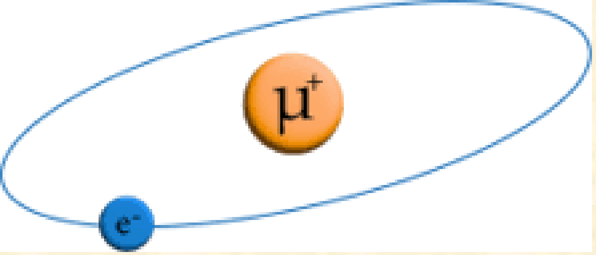

Radiative–Recoil Diagrams at Order $\alpha^2(Z\alpha)^5$

Plan 1: Evaluate the four-denominator and possibly the five-denominator integrals analytically. These are the ones whose coefficients have the highest inverse powers of x, $(1-x)$, and ϵ. Evaluate the six- through eight-denominator integrals numerically via sector decomposition followed by numerical integration, using either FIESTA or pySecDec, which handle the expansion in ϵ automatically. Problems: The analytical evaluations are time consuming and must be done individually. The numerical evaluation of the remaining integrals must be done one by one, and it might be difficult to achieve the needed precision for x near 0 or 1.

Plan 2: Evaluate all master integrals using the recently-developed “auxiliary mass flow” method. The package “AMFlow” evaluates all required integrals automatically. It handles the expansion in ϵ and allows numerical evaluation to arbitrarily high precision.

Plan 2 is by far the best!

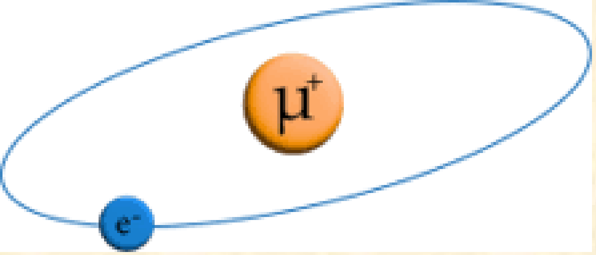

psas_2026

Radiative – Recoil Diagrams at Order $\alpha^2(Z\alpha)^5$

Plan 1: Evaluate the four-denominator and possibly the five-denominator integrals analytically. These are the ones whose coefficients have the highest inverse powers of *x*, *(1-x),* and ϵ. Evaluate the six- through eight-denominator integrals numerically via sector decomposition followed by numerical integration, using either FIESTA or pySecDec, which handle the expansion in ϵ automatically. Problems: The analytical evaluations are time consuming and must be done individually. The numerical evaluation of the remaining integrals must be done one by one, and it might be difficult to achieve the needed precision for *x* near 0 or 1.

Plan 2: Evaluate all master integrals using the recently-developed “auxiliary mass flow” method. The package “AMFlow” evaluates all required integrals automatically. It handles the expansion in ϵ and allows numerical evaluation to arbitrarily high precision.

Plan 2 is by far the best! arXiv: 2201.11669 [hep-ph]
X. Liu and Y.-Q. Ma, Comp. Phys. Comm. **283**, 108665 (2023)

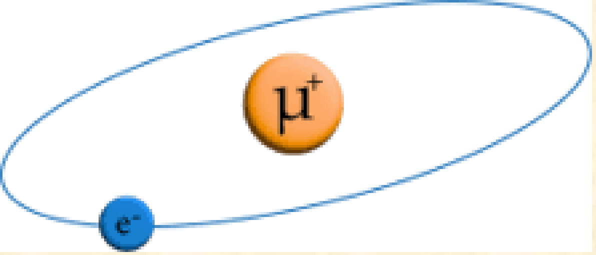

psas_2026

Radiative – Recoil Diagrams at Order $\alpha^2(Z\alpha)^5$

The required master integrals were evaluated numerically using the recently developed routine AMFlow. In the AMFlow method, an auxiliary mass term is added to the denominators. As an example, consider the integral

$$I(x) = \Phi \int \frac{d^d q}{(2\pi)^d} \left[(-q^2)(-q^2 + 2xqn)\right]^{-1}$$

where $\Phi = -i(4\pi)^{2-\epsilon} e^{\epsilon\gamma_E}$ and $n = (1, \vec{0})$ is a timelike unit vector. Augment *I* by adding an auxiliary mass to each denominator:

$$\bar{I}(x,\eta) = \Phi \int \frac{d^d q}{(2\pi)^d} \left[(-q^2 + \eta)(-q^2 + 2xqn + \eta)\right]^{-1}$$

We take the derivative of $\bar{I}(x,\eta)$ with respect to the auxiliary mass and use integration by parts to find a set of coupled first order differential equations involving $\bar{I}(x,\eta)$.

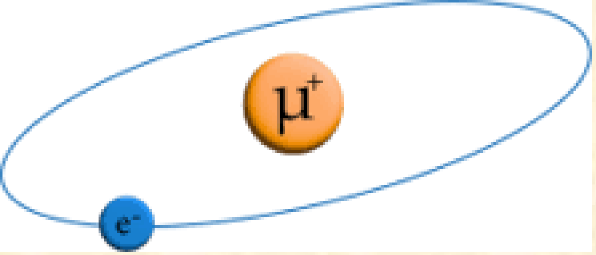

psas_2026

Radiative–Recoil Diagrams at Order $\alpha^2(Z\alpha)^5$

With the inclusion of $I_0(\eta) = \Phi \int \frac{d^dq}{(2\pi)^d}\left[(-q^2+\eta)\right]^{-1}$

and the definition $\vec{I}(x,\eta) = \begin{pmatrix} I_0(\eta) \\ \bar{I}(x,\eta) \end{pmatrix}$ we find the first order coupled

differential equation $\frac{d\vec{I}(x,\eta)}{d\eta} = M \cdot \vec{I}(x,\eta)$

where $M = \begin{pmatrix} \frac{1-\epsilon}{x^2+\eta} & 0 \\ \frac{1-\epsilon}{2\pi(x^2+\eta)} & \frac{1-2\epsilon}{2\eta} \end{pmatrix}$

This first order linear differential equation can be solved using power series. The boundary condition is conveniently found at $\eta = \infty$.

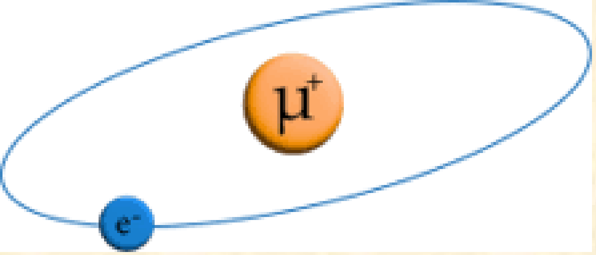

Radiative – Recoil Diagrams at Order $\alpha^2(Z\alpha)^5$

As η approaches ∞, we have $q^2 \sim \eta, \quad x << \sqrt{\eta}$ and we can expand

$$\bar{I}(x,\eta) = \Phi \int \frac{d^d q}{(2\pi)^d} \frac{1}{-q^2 + 2xqn + \eta}$$

$$= \Phi \int \frac{d^d q}{(2\pi)^d} \frac{1}{(-q^2+\eta)\left(1 + \frac{2xqn}{-q^2+\eta}\right)}$$

$$= \Phi \int \frac{d^d q}{(2\pi)^d} \frac{1}{(-q^2+\eta)} \left\{ 1 - \frac{2xqn}{-q^2+\eta} + \left(\frac{2xqn}{-q^2+\eta}\right)^2 + \cdots \right\}$$

In this limit, the integrals needed are vacuum integrals and are well understood, so the boundary conditions are known. The DEs are solved by the series method, and analytically continued from $\eta \sim \infty$ to $\eta \to -i0$. Enough terms in the series are used in order to obtain the desired precision.

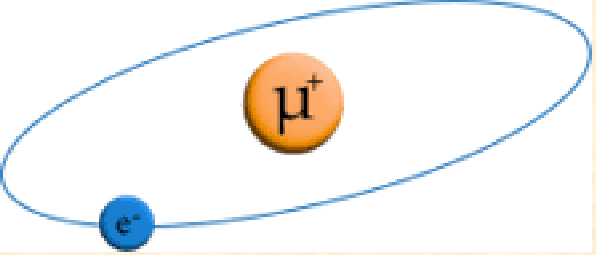

Radiative – Recoil Diagrams at Order $\alpha^2(Z\alpha)^5$

In practice, the auxiliary mass term is added to only a subset of the denominators. This reduces significantly the number of integrals that must be included in the coupled differential equations, but makes the evaluation of the boundary conditions more involved. The boundary conditions now require the evaluation of a number of additional integrals. These additional integrals are themselves evaluated using auxiliary mass flow. The AMFlow program handles the recursive aspect of the algorithm automatically. In the process, many hundreds of coupled differential equations are produced and solved, all without user intervention.

Radiative – Recoil Diagrams at Order $\alpha^2(Z\alpha)^5$

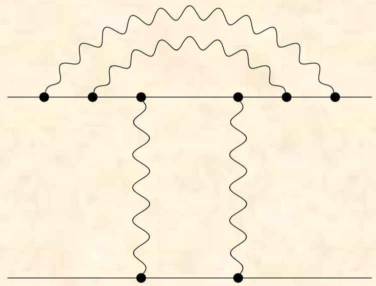

Radiative-recoil at order $$\frac{m_e\alpha^2(Z\alpha)^5}{n^3}\left(\frac{m_r}{m_e}\right)^3\left(\frac{m_e}{m_\mu}\right)$$

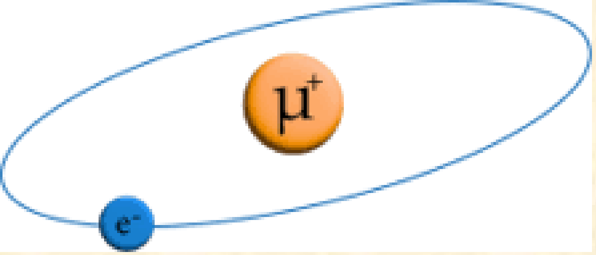

Radiative – Recoil Diagrams at Order $\alpha^2(Z\alpha)^5$

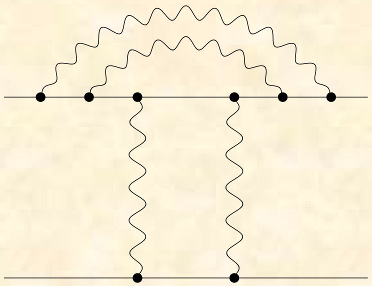

Radiative-recoil at order $\dfrac{m_e\alpha^2(Z\alpha)^5}{n^3}\left(\dfrac{m_r}{m_e}\right)^3\left(\dfrac{m_e}{m_\mu}\right)$

For the average correction $\Delta E_{\rm avg} = (3\Delta E_{s=1} + \Delta E_{s=0})/4$

we define $\Delta E_{\rm avg} = \dfrac{m_1\alpha^2(Z\alpha)^5}{\pi n^3}\left(\dfrac{m_r}{m_1}\right)^3\Big(-R_{\rm avg}(x)\Big)$ where $x = \dfrac{m_1}{m_2}$,

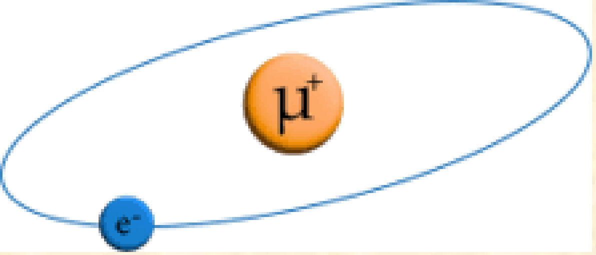

Radiative – Recoil Diagrams at Order $\alpha^2(Z\alpha)^5$

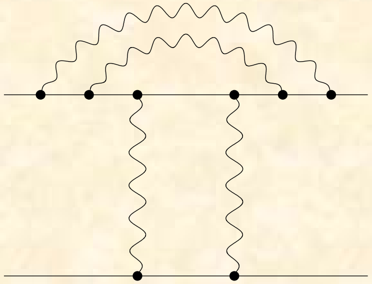

Radiative-recoil at order $\dfrac{m_e\alpha^2(Z\alpha)^5}{n^3}\left(\dfrac{m_r}{m_e}\right)^3\left(\dfrac{m_e}{m_\mu}\right)$

For the average correction $\Delta E_{\rm avg} = (3\Delta E_{s=1} + \Delta E_{s=0})/4$

we define $\Delta E_{\rm avg} = \dfrac{m_1\alpha^2(Z\alpha)^5}{\pi n^3}\left(\dfrac{m_r}{m_1}\right)^3\Big(-R_{\rm avg}(x)\Big)$ where $x = \dfrac{m_1}{m_2}$,

and for the hyperfine splitting $\Delta E_{\rm hfs} = \Delta E_{s=1} - \Delta E_{s=0}$

we define $\Delta E_{\rm hfs} = \dfrac{\alpha^2(Z\alpha)}{\pi n^3}\tilde{E}_F\Big(-R_{\rm hfs}(x)\Big)$

where $\tilde{E}_F \equiv \dfrac{8(Z\alpha)^4}{3}\left(\dfrac{m_r}{m_1}\right)^3\left(\dfrac{m_1}{m_2}\right)m_1$

Radiative–Recoil Diagrams at Order $\alpha^2(Z\alpha)^5$

We evaluated all 139 required master integrals using AMFlow. All eight orders in the dimensional regularization parameters were evaluated at once. The results were done to 42 significant figures.

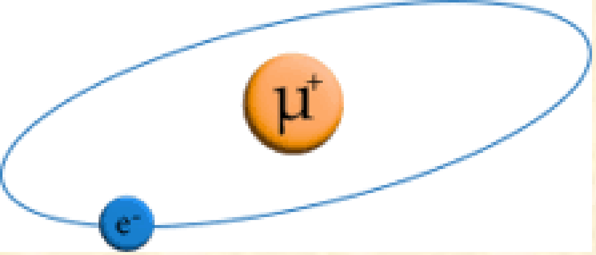

Radiative – Recoil Diagrams at Order $\alpha^2(Z\alpha)^5$

We evaluated all 139 required master integrals using AMFlow. All eight orders in the dimensional regularization parameters were evaluated at once. The results were done to 42 significant figures.

Each of the master integrals was multiplied by the appropriate coefficient to give the full scattering amplitude

$$\mathcal{M} = \sum_{k=1}^{139} A_k(x,\epsilon)\, I_k(x,\epsilon)\ ,$$

Radiative – Recoil Diagrams at Order $\alpha^2(Z\alpha)^5$

We evaluated all 139 required master integrals using AMFlow. All eight orders in the dimensional regularization parameters were evaluated at once. The results were done to 42 significant figures.

Each of the master integrals was multiplied by the appropriate coefficient to give the full scattering amplitude

$$\mathcal{M} = \sum_{k=1}^{139} A_k(x,\epsilon)\, I_k(x,\epsilon) \; ,$$

Checks: $1/\epsilon^7$, $1/\epsilon^6$, $1/\epsilon^5$, $1/\epsilon^4$ terms all vanished.

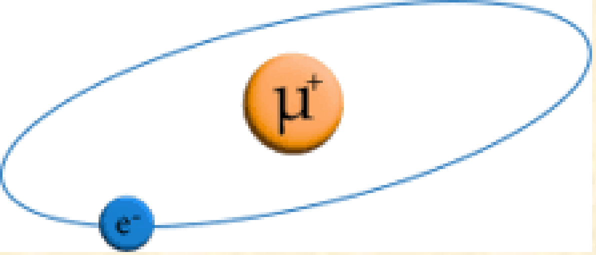

psas_2026

Radiative – Recoil Diagrams at Order $\alpha^2(Z\alpha)^5$

We evaluated all 139 required master integrals using AMFlow. All eight orders in the dimensional regularization parameters were evaluated at once. The results were done to 42 significant figures.

Each of the master integrals was multiplied by the appropriate coefficient to give the full scattering amplitude

$$\mathcal{M} = \sum_{k=1}^{139} A_k(x,\epsilon)\, I_k(x,\epsilon) \ ,$$

Checks: $1/\epsilon^7$, $1/\epsilon^6$, $1/\epsilon^5$, $1/\epsilon^4$ terms all vanished. Next, the renormalization procedure was implemented. After renormalization, all $1/\epsilon^3$, $1/\epsilon^2$, $1/\epsilon$ terms vanished, leaving a finite result.

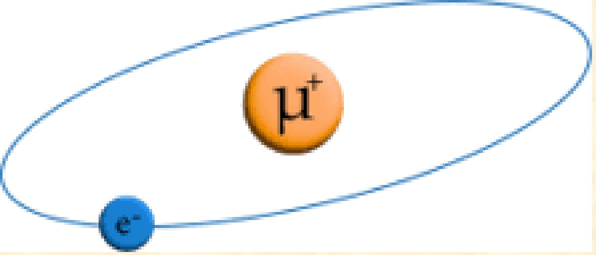

Radiative – Recoil Diagrams at Order $\alpha^2(Z\alpha)^5$

We evaluated all 139 required master integrals using AMFlow. All eight orders in the dimensional regularization parameters were evaluated at once. The results were done to 42 significant figures.

Each of the master integrals was multiplied by the appropriate coefficient to give the full scattering amplitude

$$\mathcal{M} = \sum_{k=1}^{139} A_k(x,\epsilon)\, I_k(x,\epsilon)\ ,$$

Checks: $1/\epsilon^7$, $1/\epsilon^6$, $1/\epsilon^5$, $1/\epsilon^4$ terms all vanished. Next, the renormalization procedure was implemented. After renormalization, all $1/\epsilon^3$, $1/\epsilon^2$, $1/\epsilon$ terms vanished, leaving a finite result.

As will be shown, our results are consistent with the known no-recoil result at x=0. As an additional check, the $x = 1$ (positronium) calculation will be done separately and compared with the $x \to 1$ limit of our results.

Radiative−Recoil Diagrams at Order $\alpha^2(Z\alpha)^5$

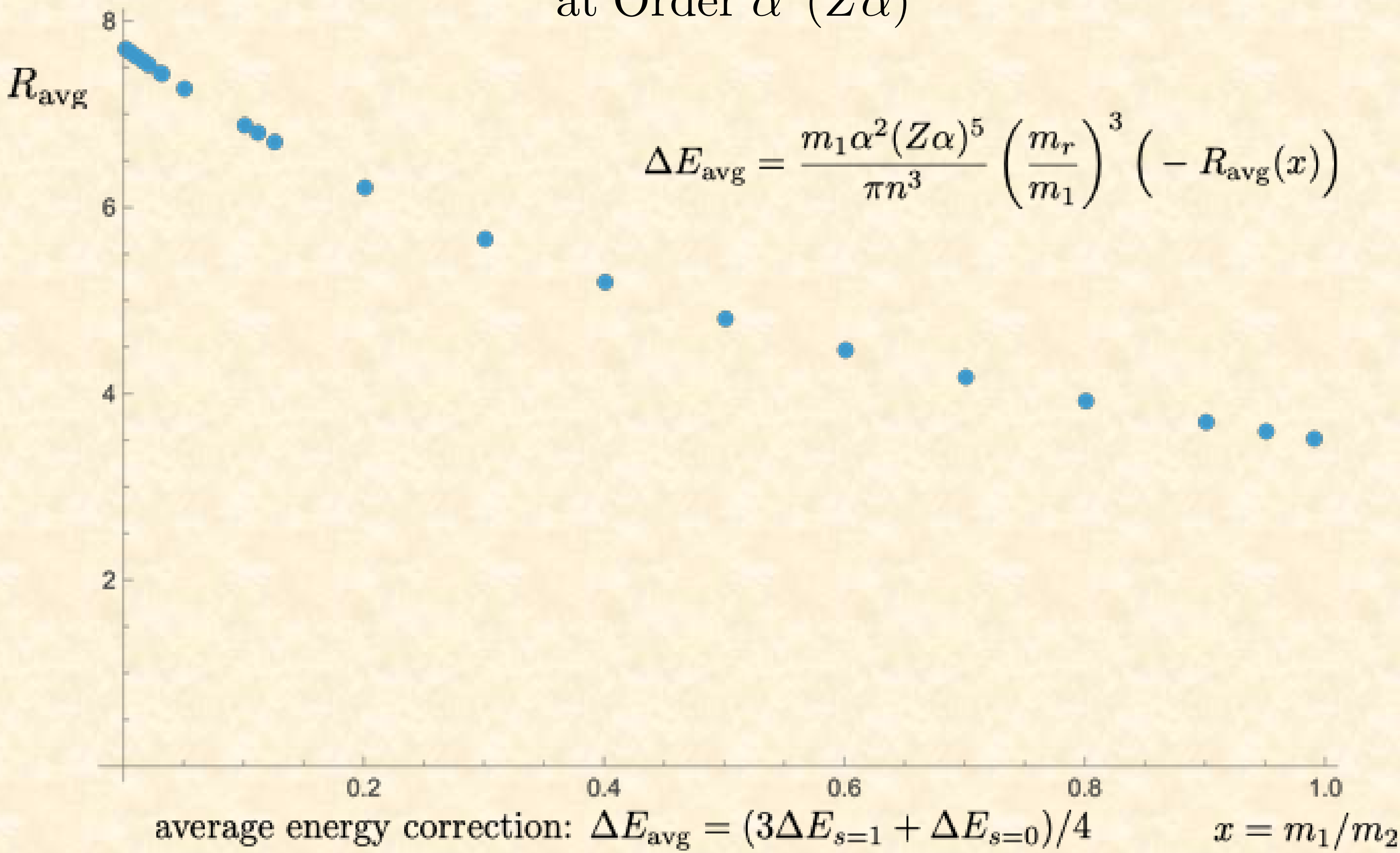

$$\Delta E_{\rm avg} = \frac{m_1 \alpha^2 (Z\alpha)^5}{\pi n^3} \left(\frac{m_r}{m_1}\right)^3 \left(-R_{\rm avg}(x)\right)$$

average energy correction: $\Delta E_{\rm avg} = (3\Delta E_{s=1} + \Delta E_{s=0})/4$

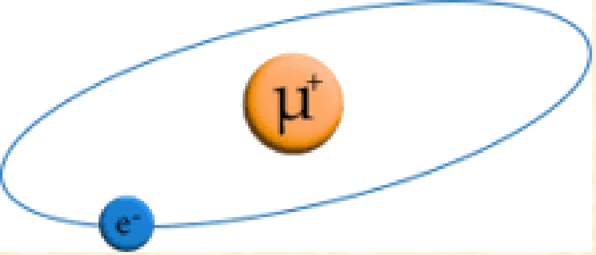

psas_2026

Radiative−Recoil Diagrams at Order $\alpha^2(Z\alpha)^5$

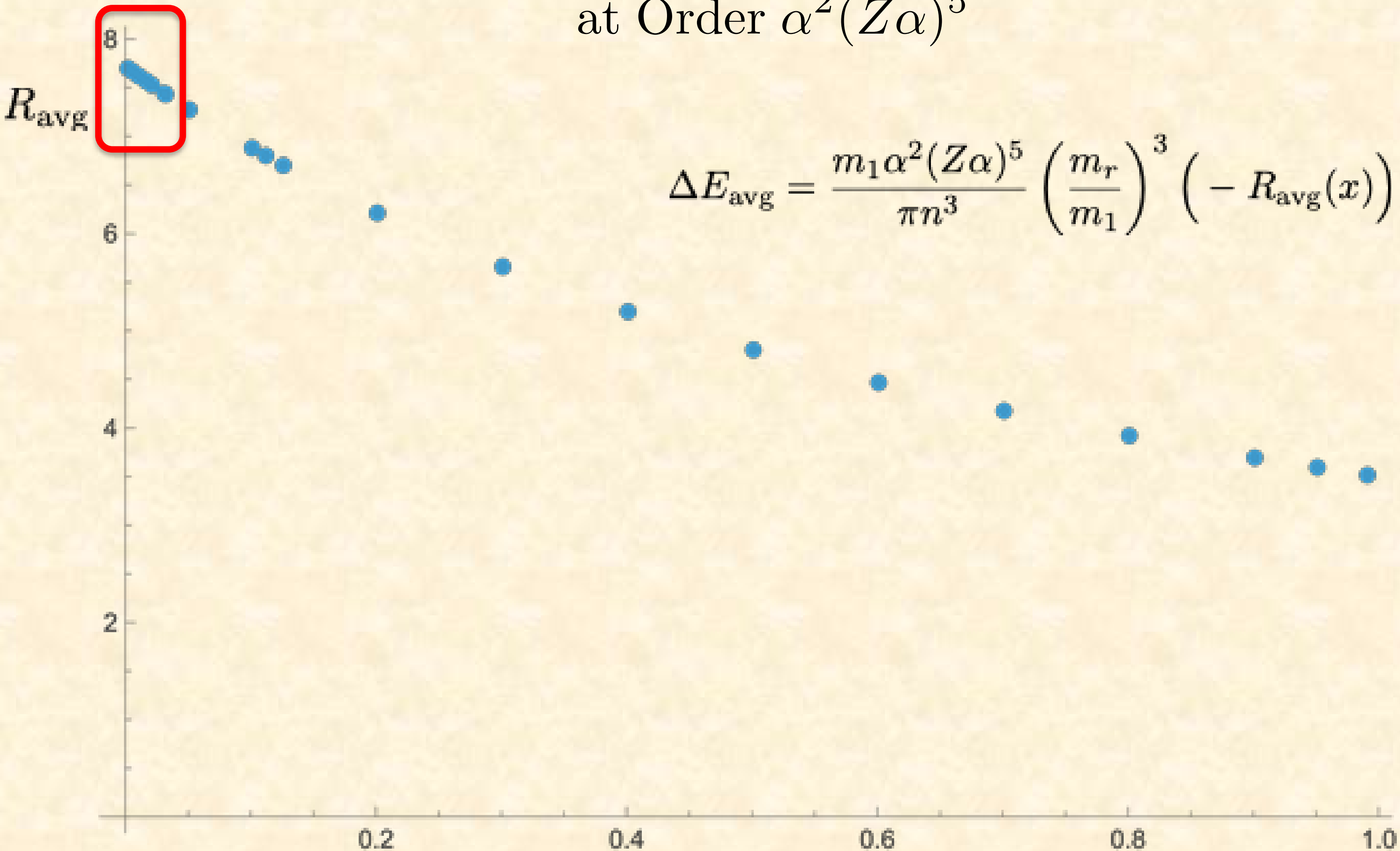

$$\Delta E_{\text{avg}} = \frac{m_1 \alpha^2 (Z\alpha)^5}{\pi n^3} \left(\frac{m_r}{m_1}\right)^3 \left(-R_{\text{avg}}(x)\right)$$

average energy correction: $\Delta E_{\text{avg}} = (3\Delta E_{s=1} + \Delta E_{s=0})/4$ $\quad x = m_1/m_2$

Radiative−Recoil Diagrams at Order $\alpha^2(Z\alpha)^5$

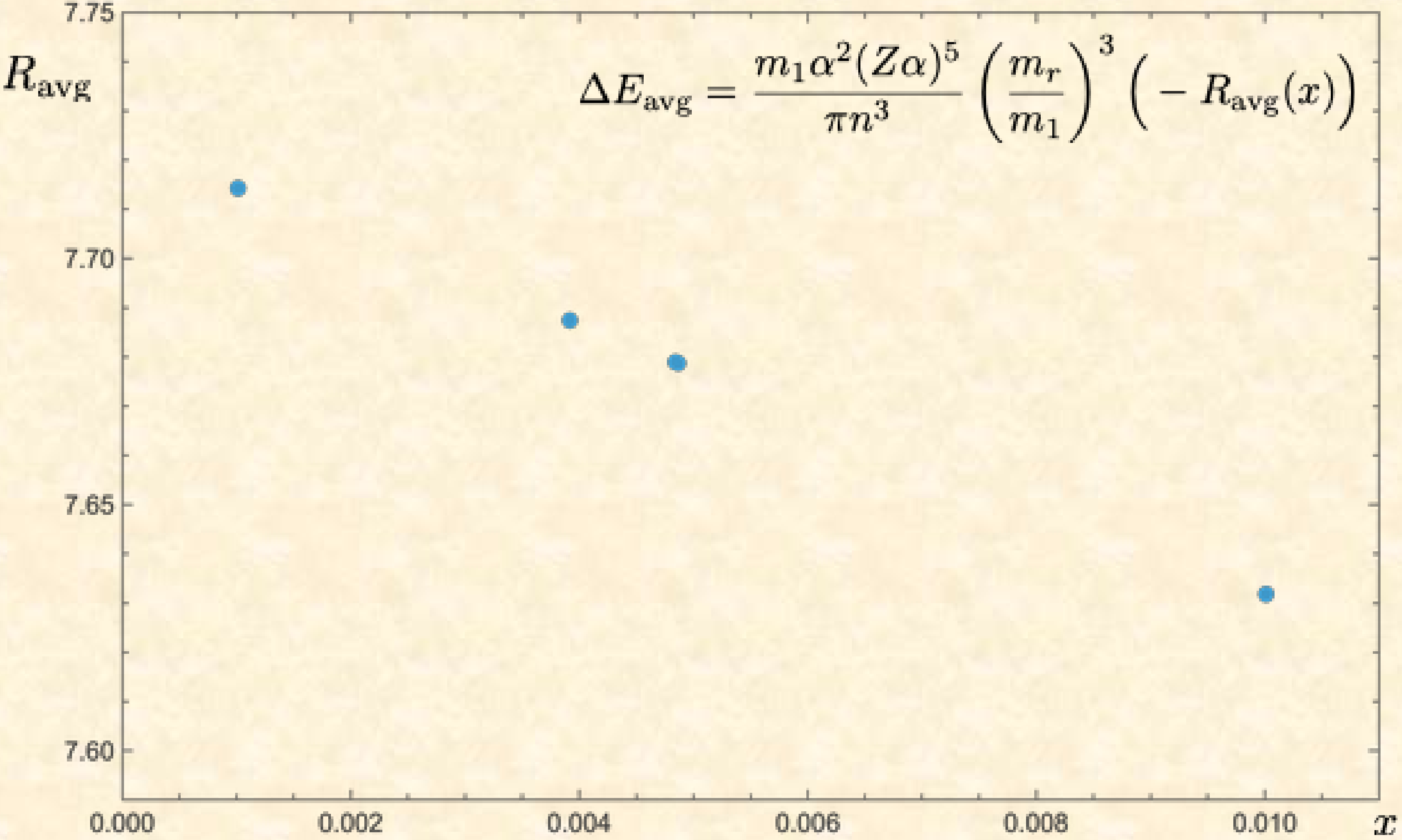

Radiative−Recoil Diagrams at Order $\alpha^2(Z\alpha)^5$

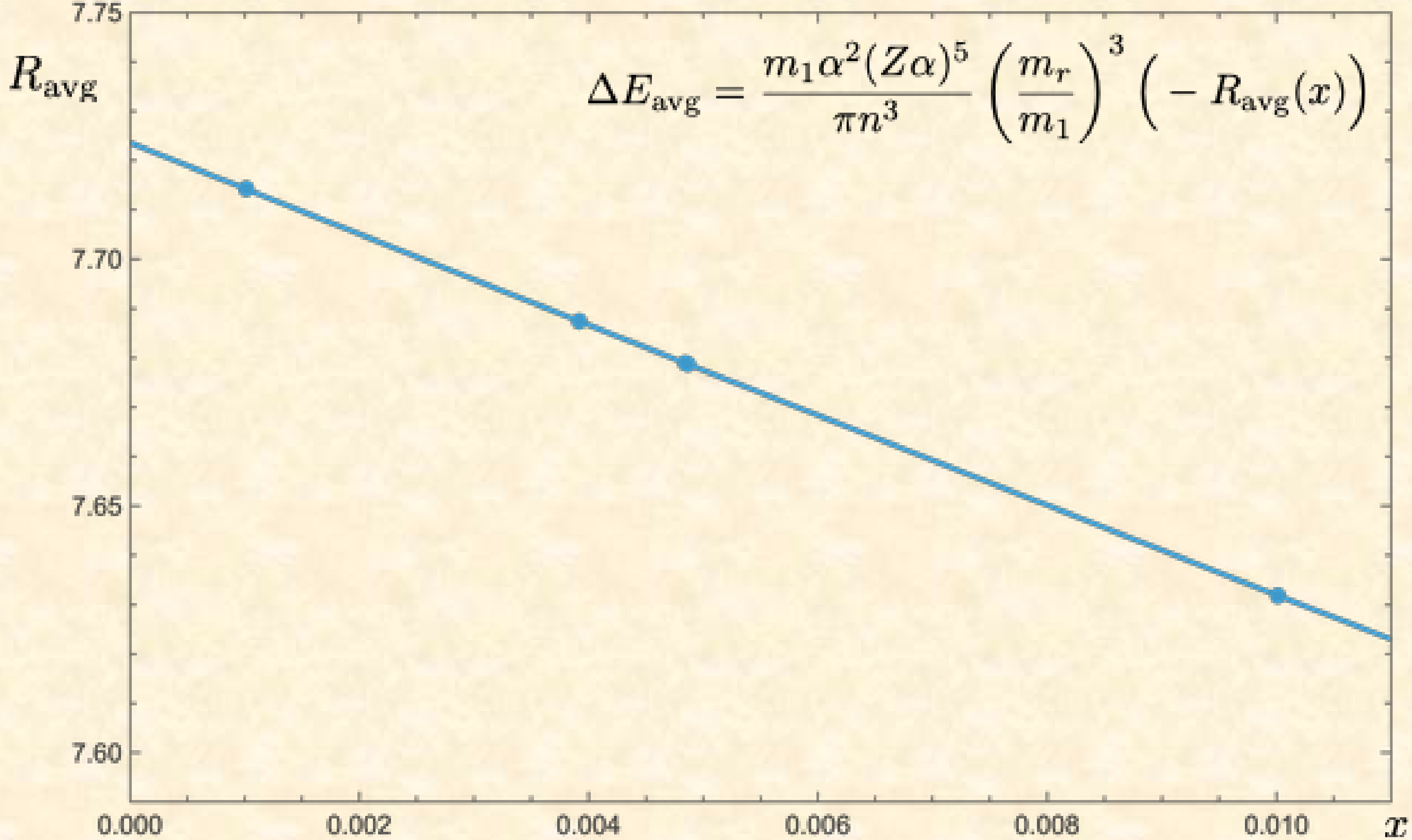

Radiative−Recoil Diagrams at Order $\alpha^2(Z\alpha)^5$

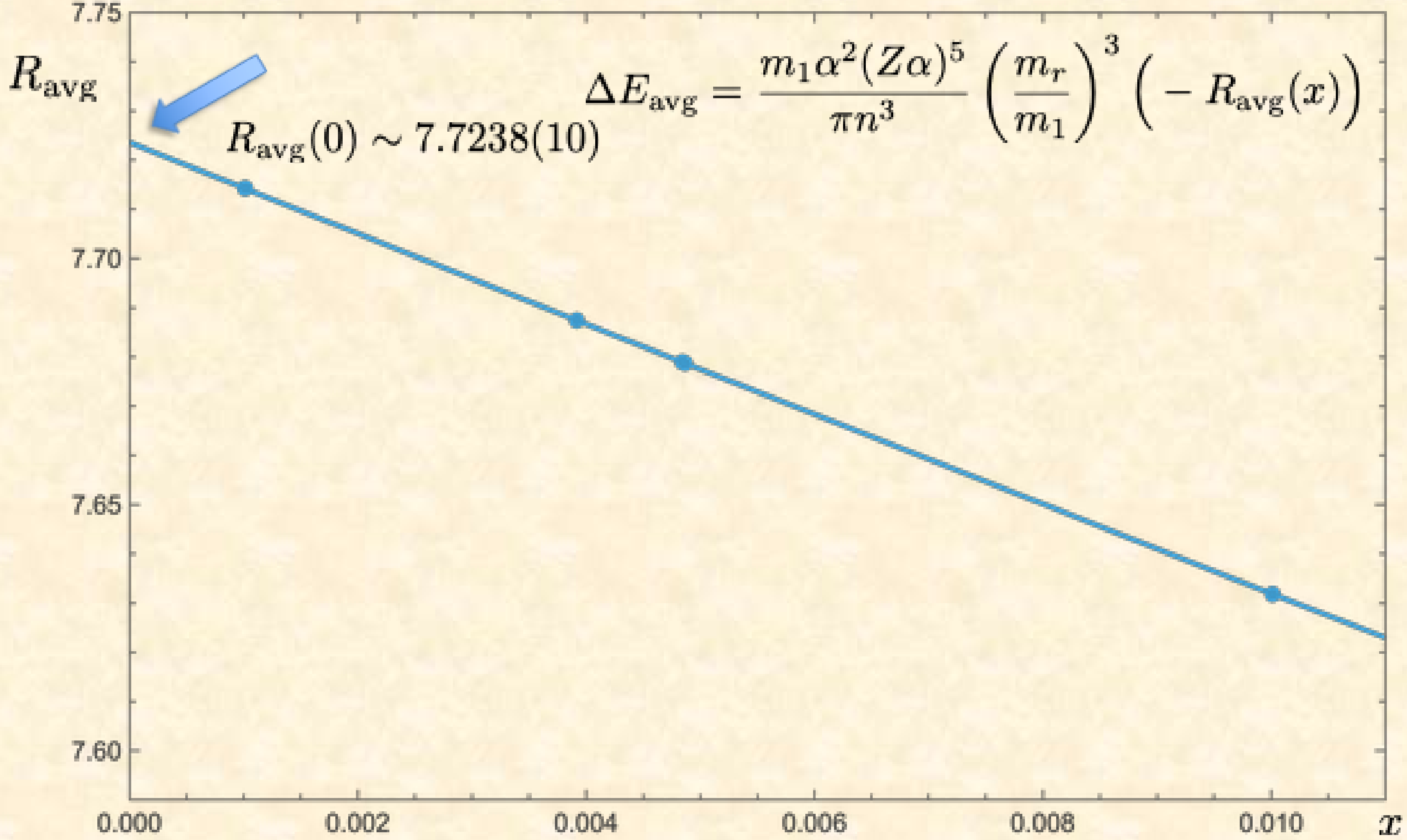

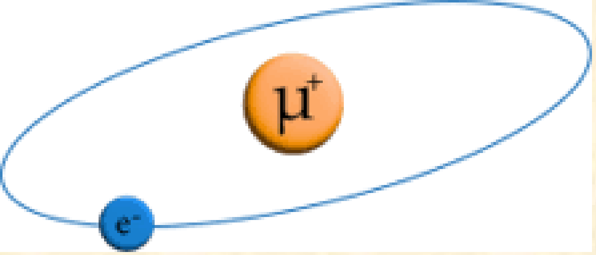

Radiative−Recoil Diagrams at Order $\alpha^2(Z\alpha)^5$

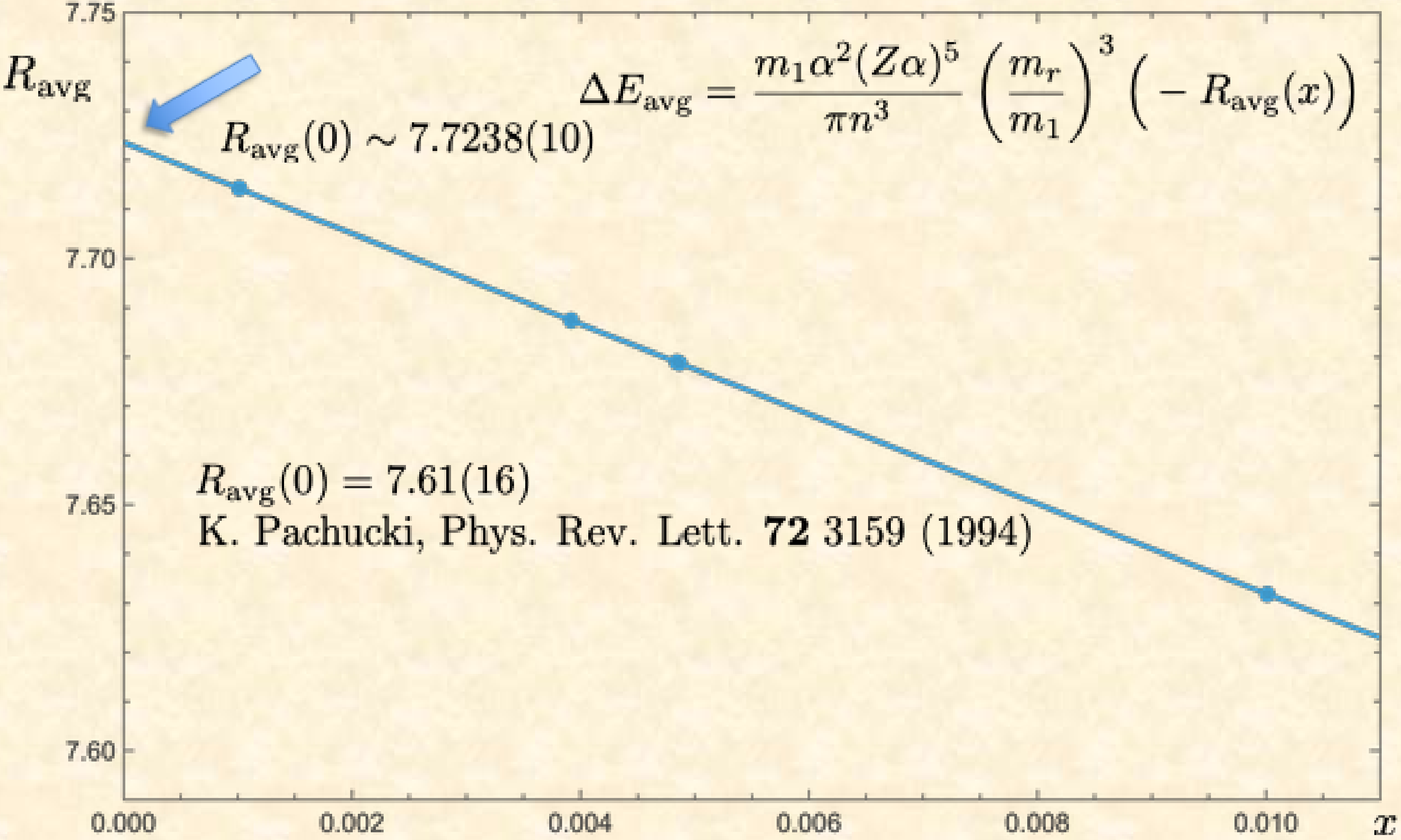

Radiative−Recoil Diagrams at Order $\alpha^2(Z\alpha)^5$

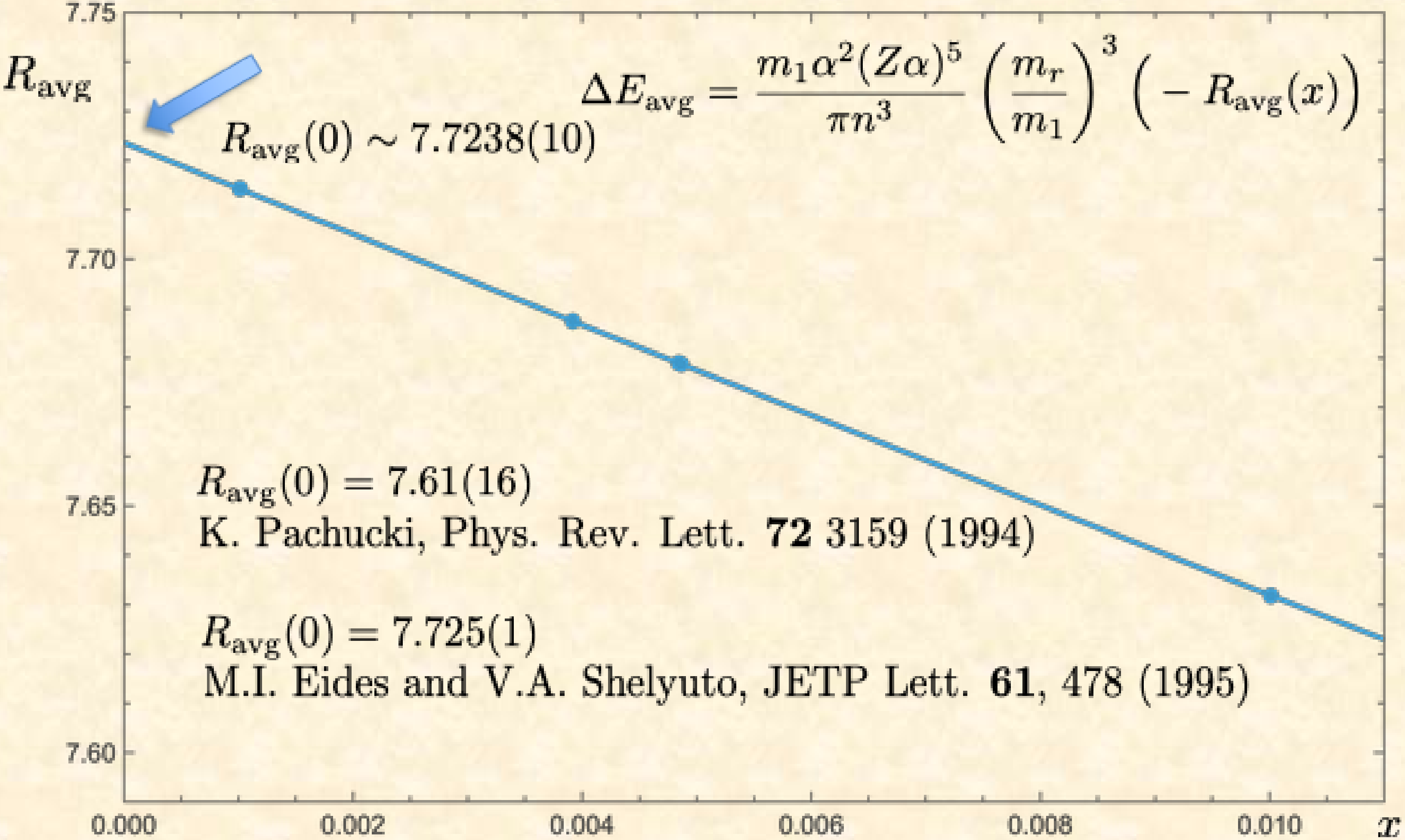

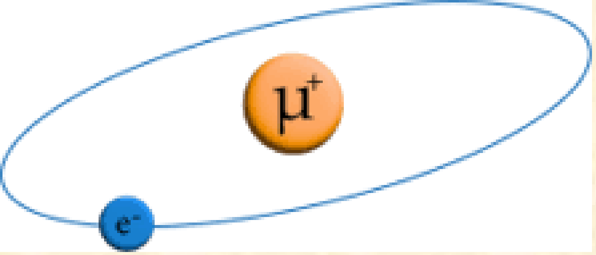

Radiative−Recoil Diagrams at Order $\alpha^2(Z\alpha)^5$

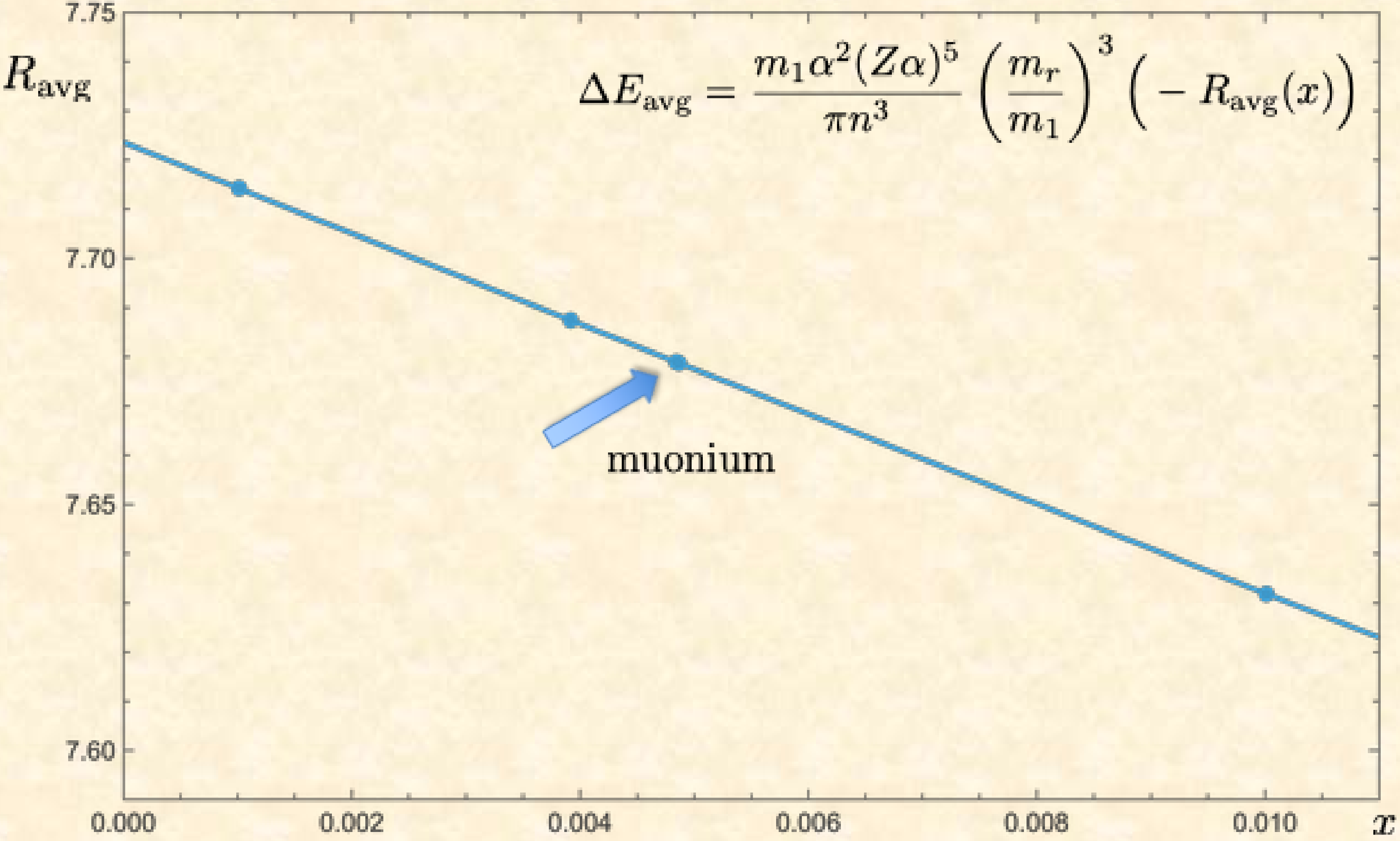

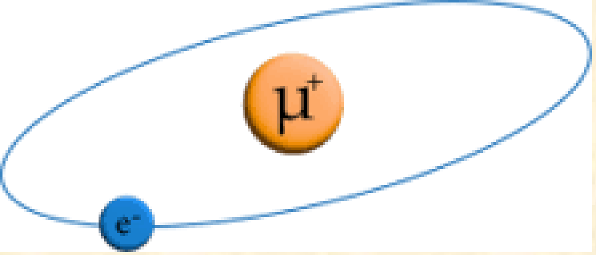

Radiative–Recoil Diagrams at Order $\alpha^2(Z\alpha)^5$

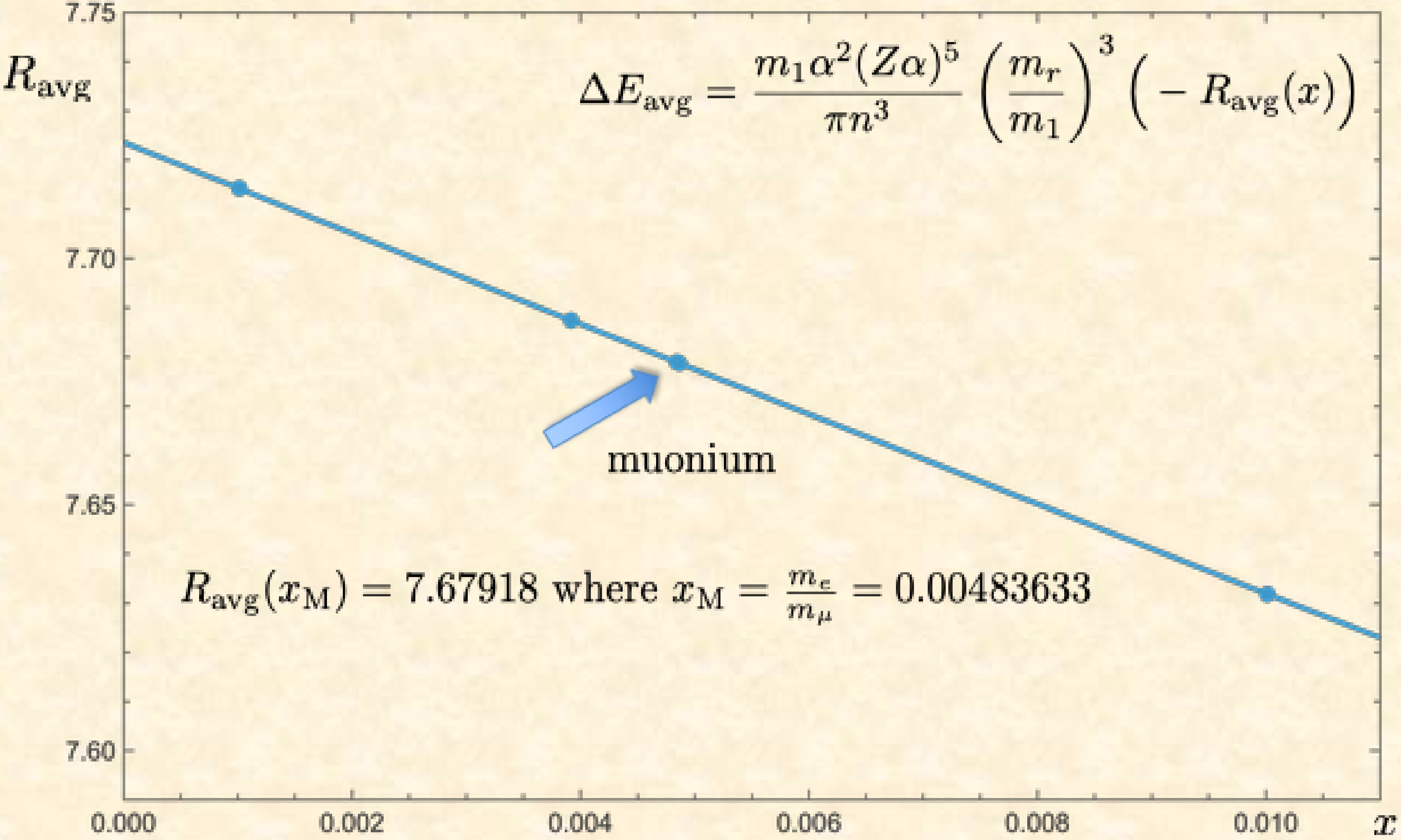

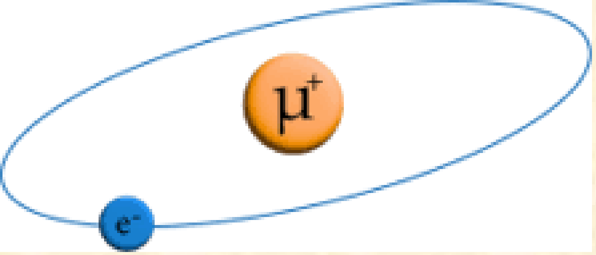

Radiative–Recoil Diagrams at Order $\alpha^2(Z\alpha)^5$

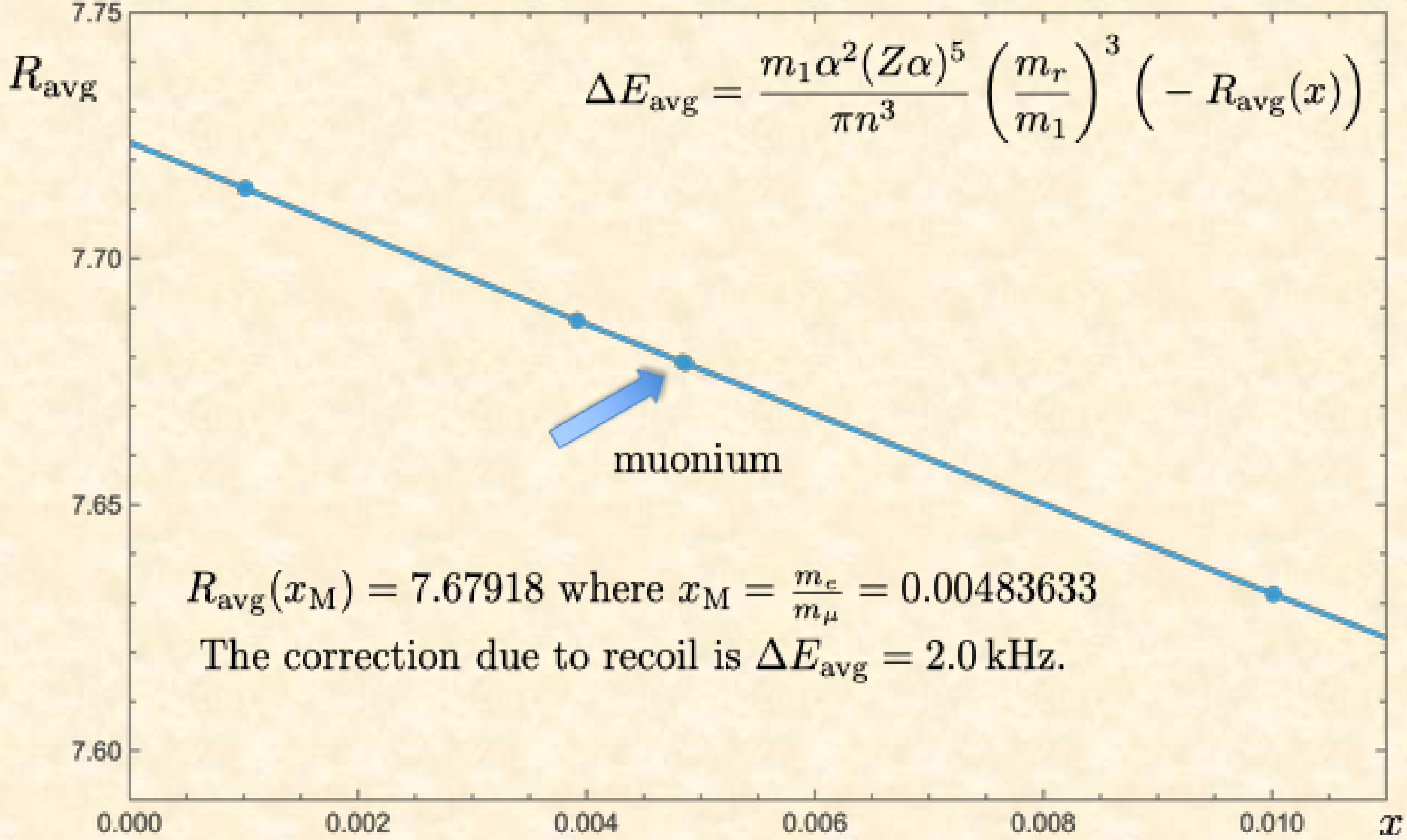

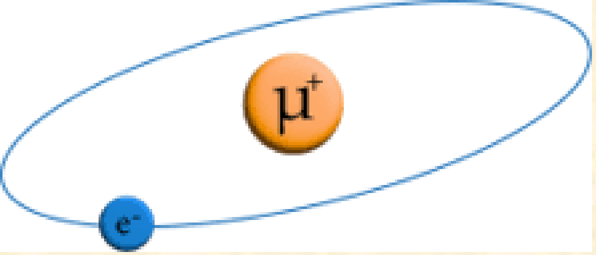

Radiative–Recoil Diagrams at Order $\alpha^2(Z\alpha)^5$

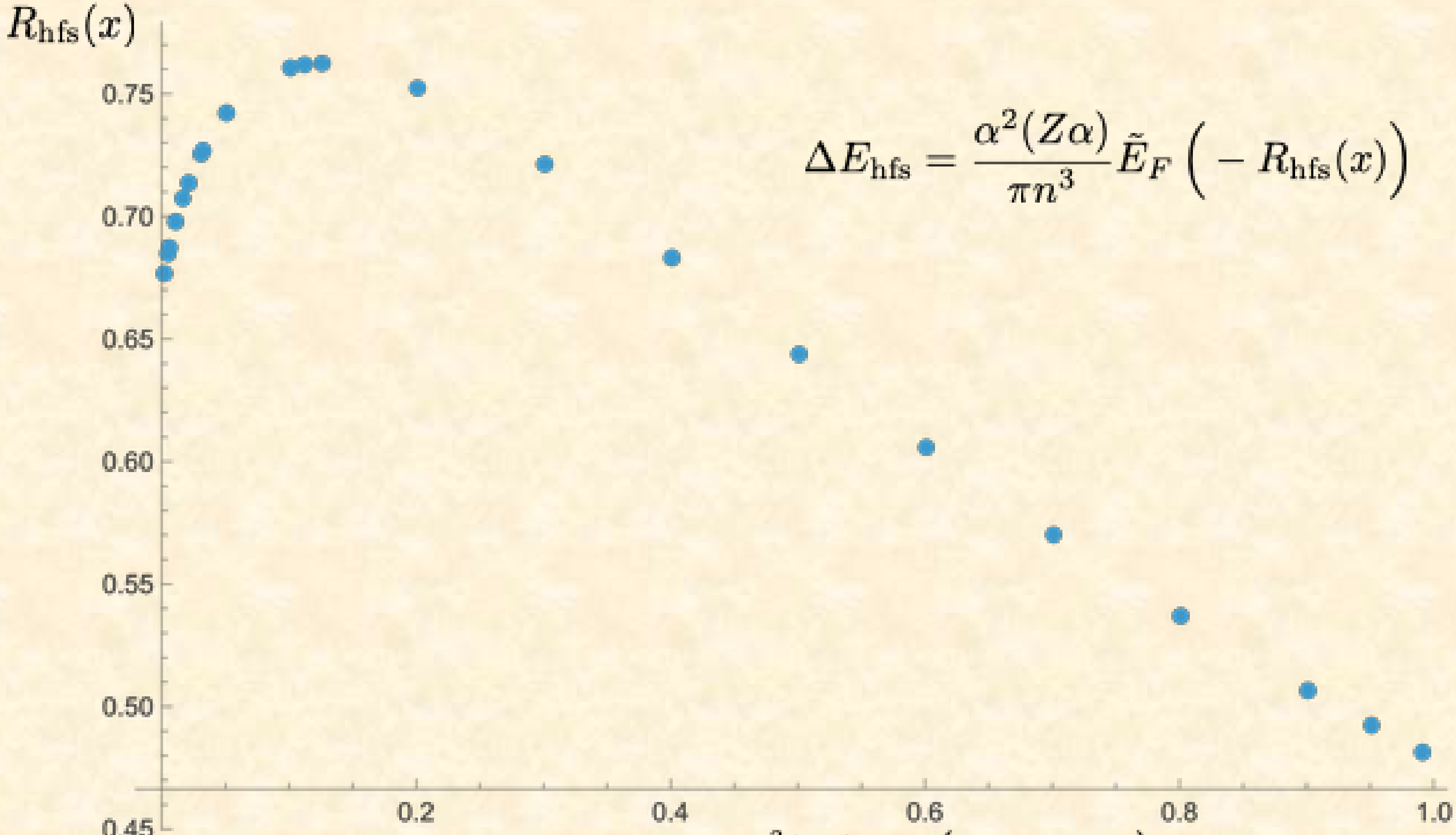

hyperfine splitting: $\Delta E_{\mathrm{hfs}} = \frac{\alpha^2(Z\alpha)}{\pi n^3}\tilde{E}_F\left(-R_{\mathrm{hfs}}(x)\right)$ $x = m_1/m_2$

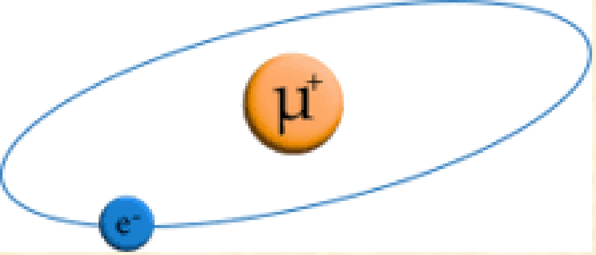

Radiative – Recoil Diagrams at Order $\alpha^2(Z\alpha)^5$

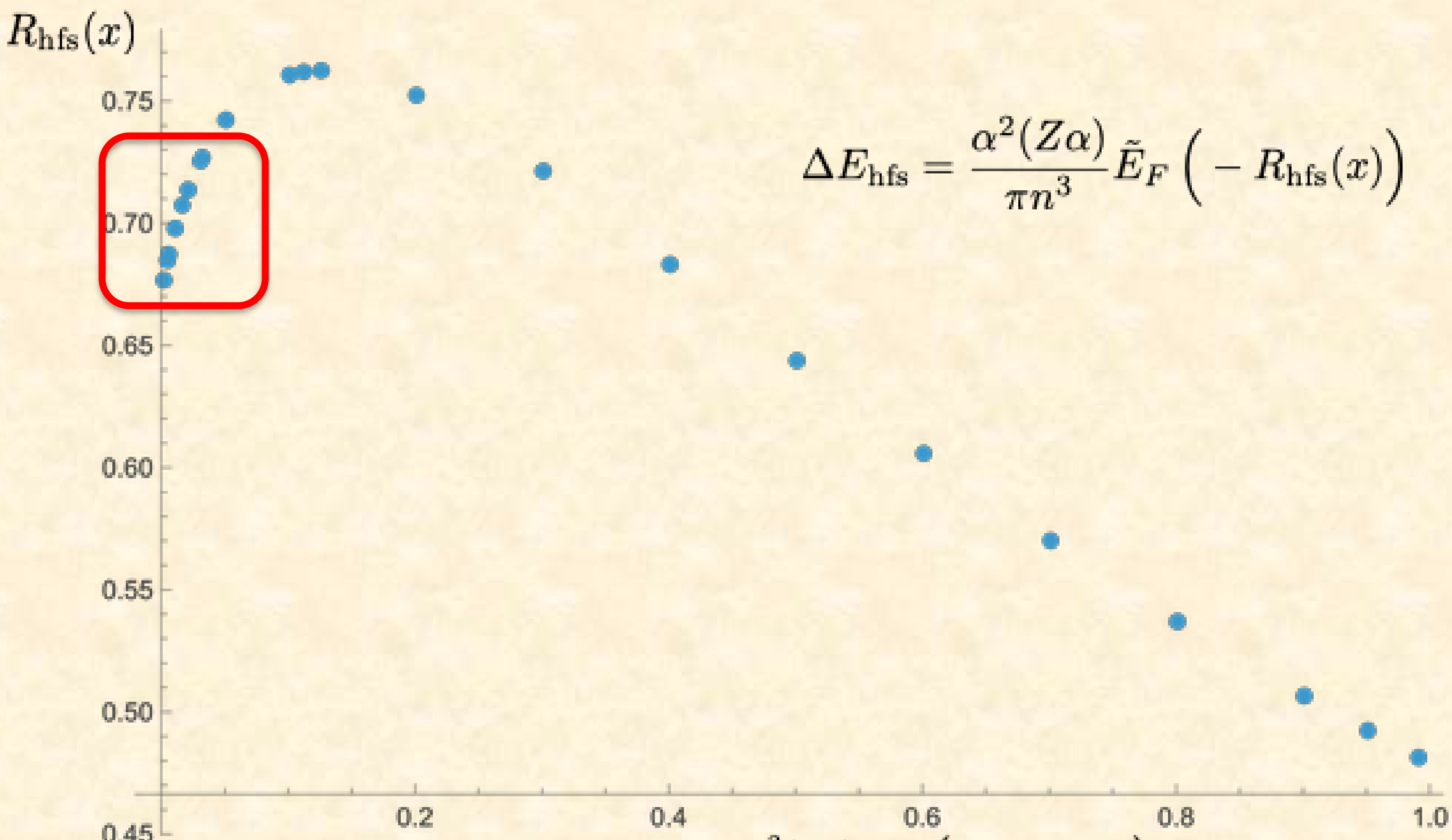

hyperfine splitting: $\Delta E_{\rm hfs} = \frac{\alpha^2(Z\alpha)}{\pi n^3}\tilde{E}_F\left(-R_{\rm hfs}(x)\right)$ $\quad x = m_1/m_2$

Radiative−Recoil Diagrams at Order $\alpha^2(Z\alpha)^5$

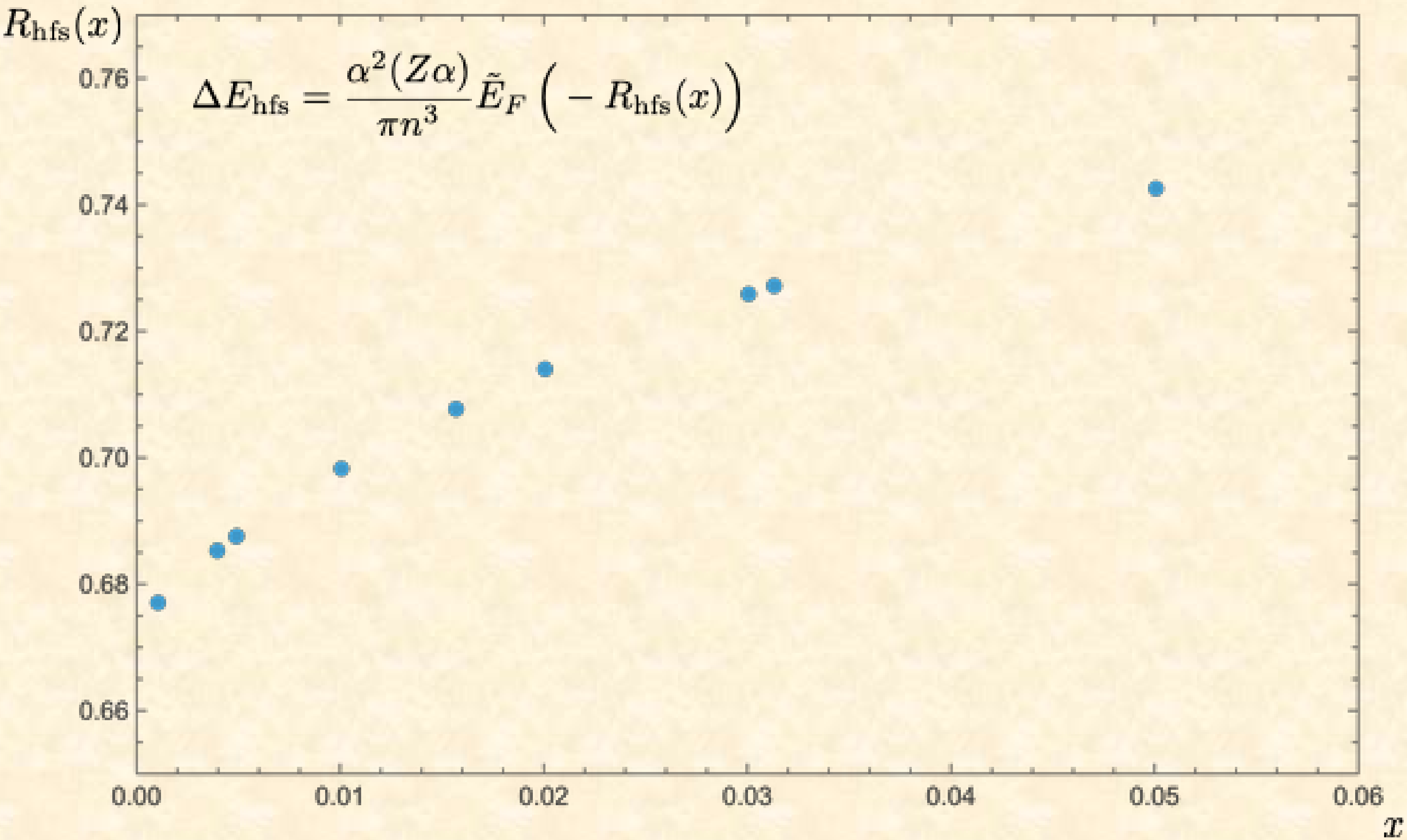

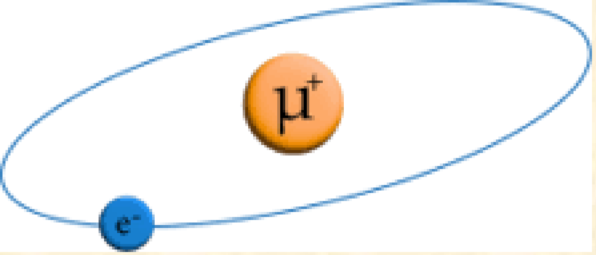

Radiative−Recoil Diagrams at Order $\alpha^2(Z\alpha)^5$

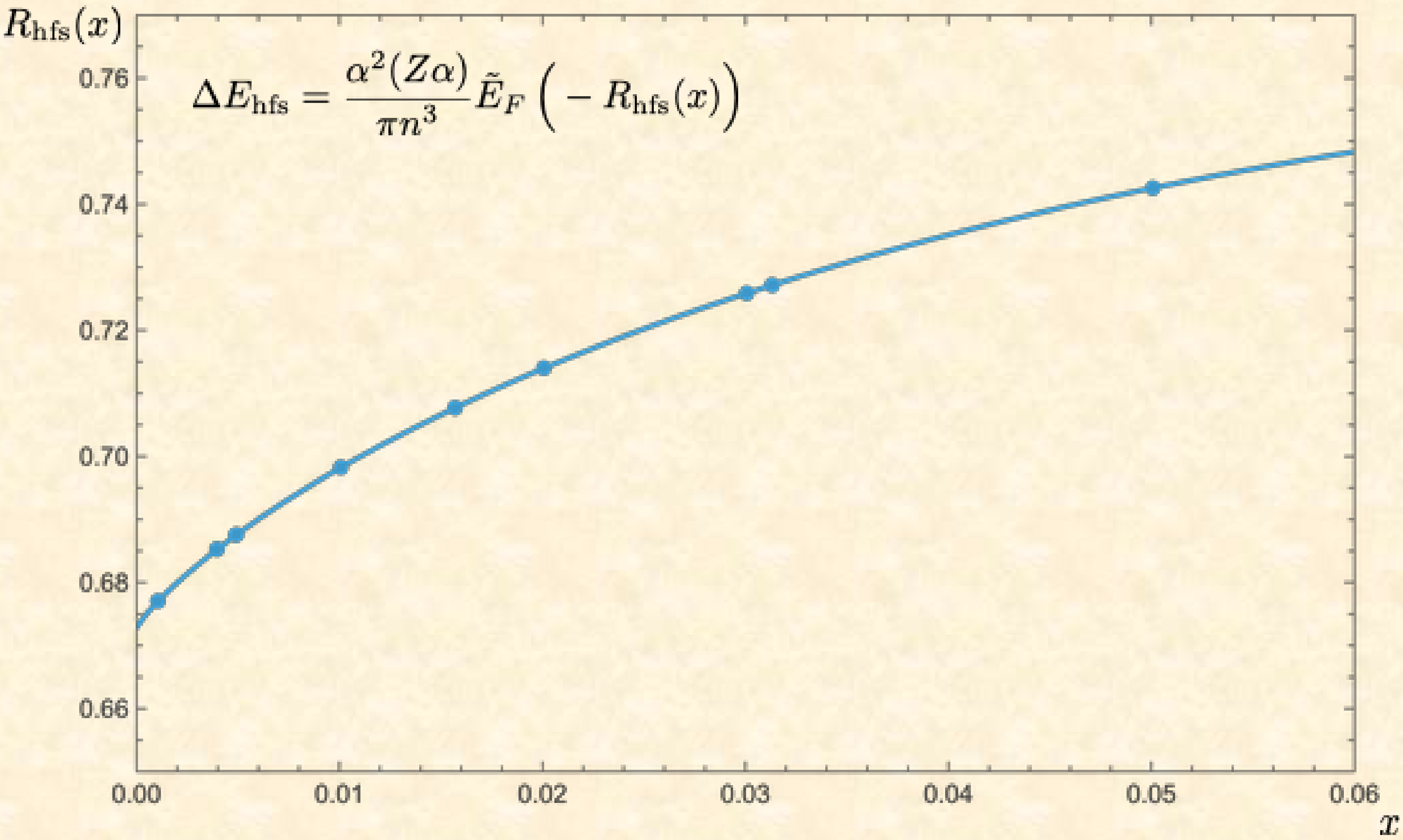

Radiative−Recoil Diagrams

at Order $\alpha^2(Z\alpha)^5$

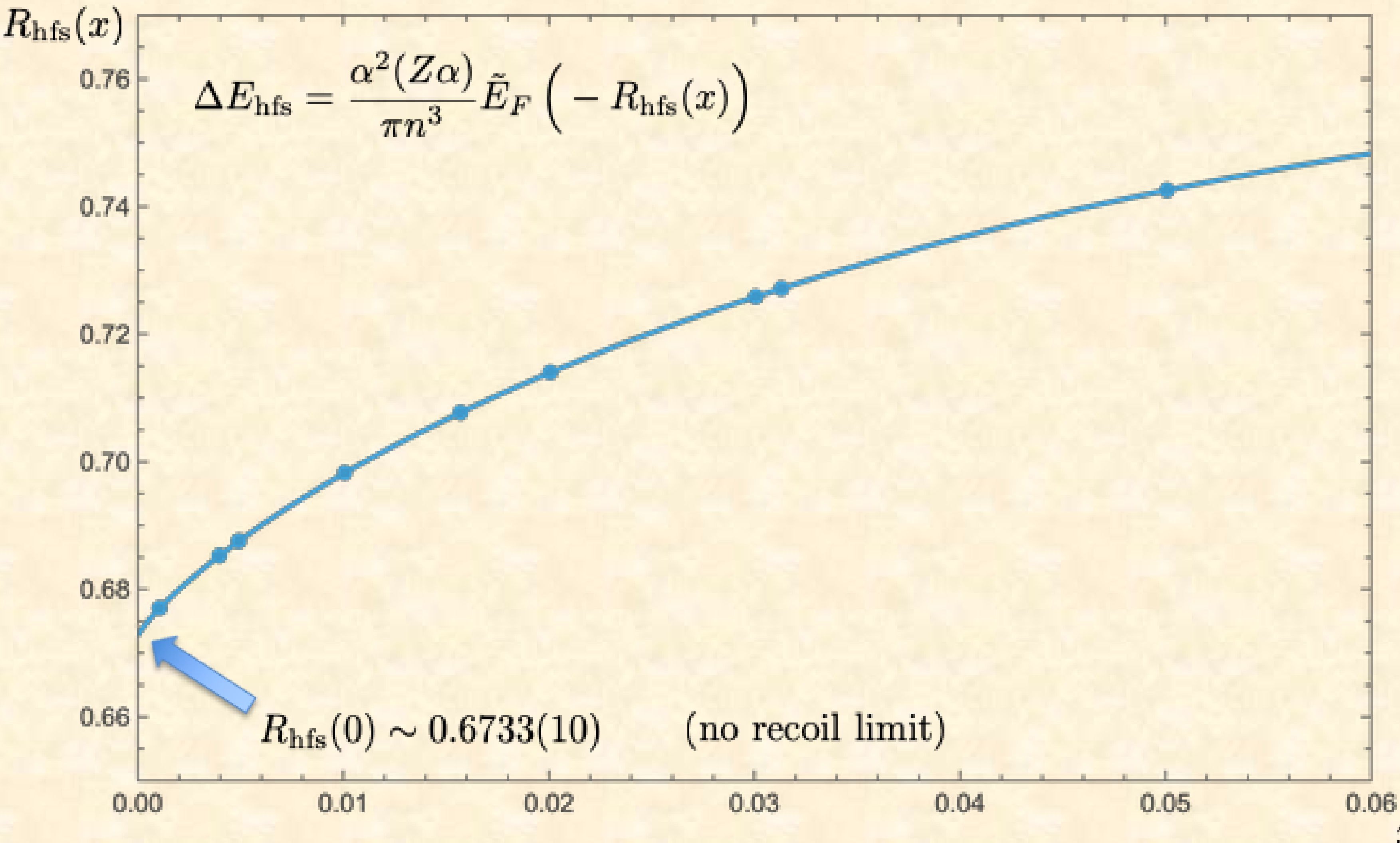

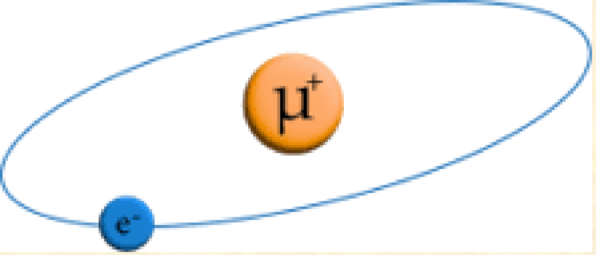

Radiative–Recoil Diagrams at Order $\alpha^2(Z\alpha)^5$

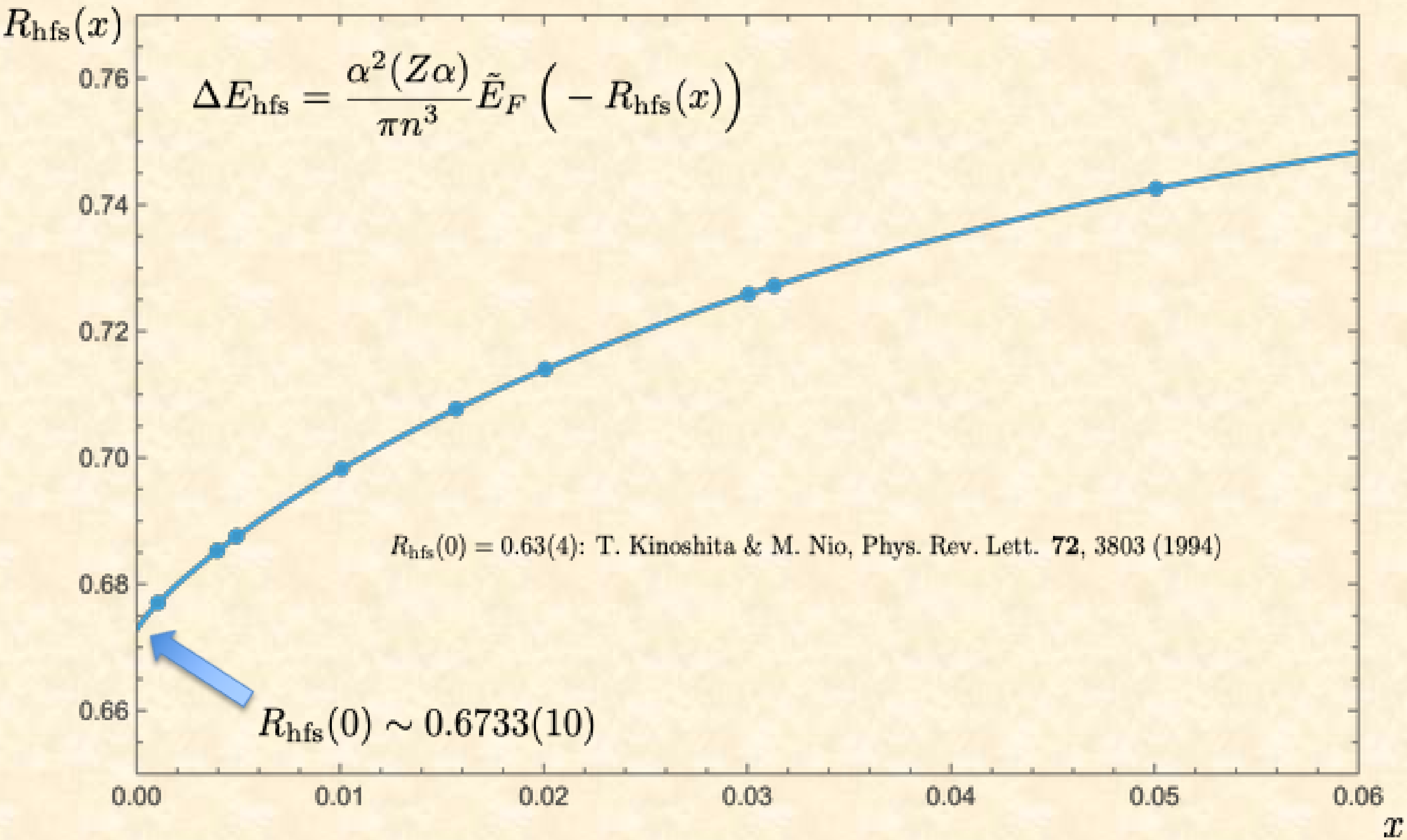

Radiative−Recoil Diagrams at Order $\alpha^2(Z\alpha)^5$

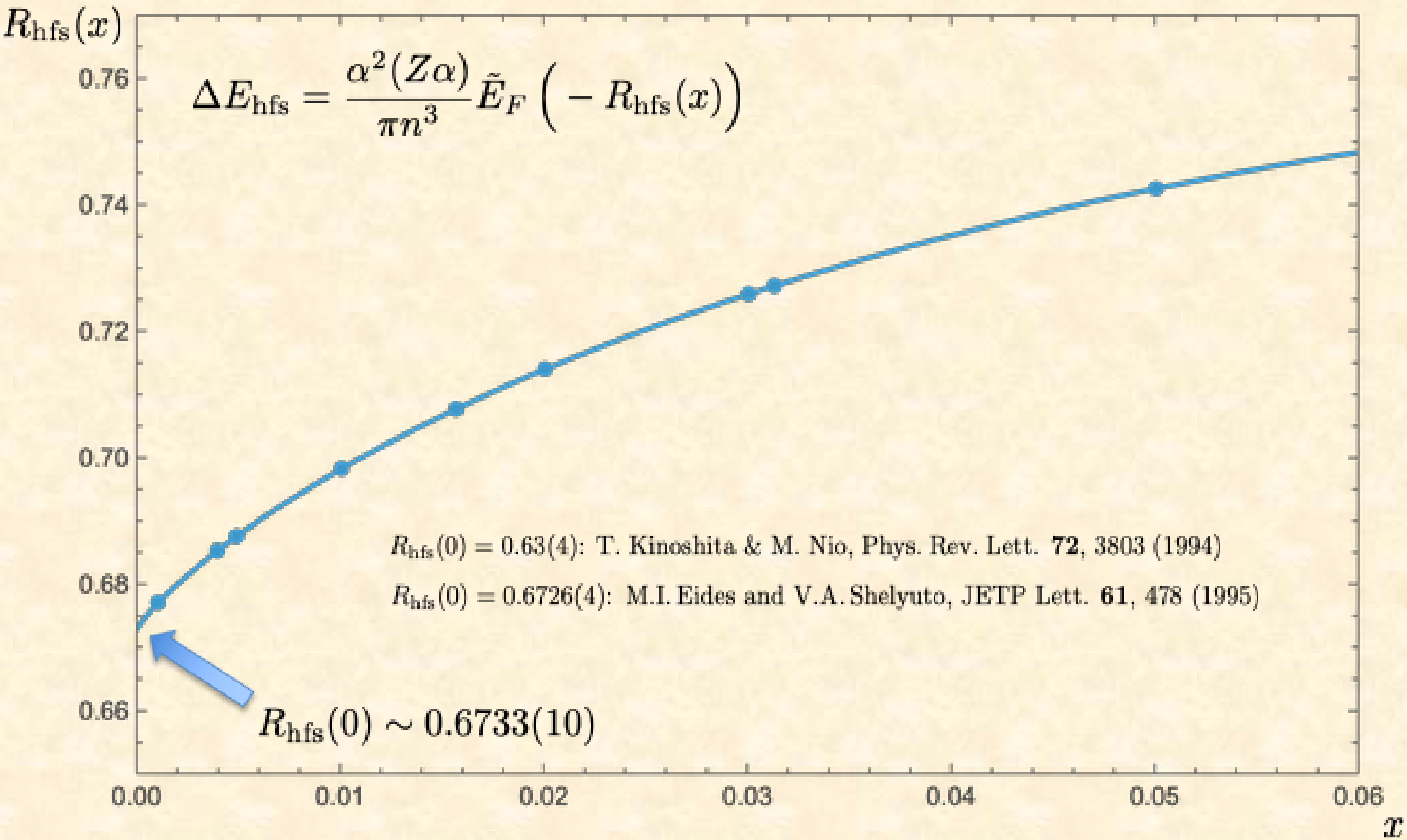

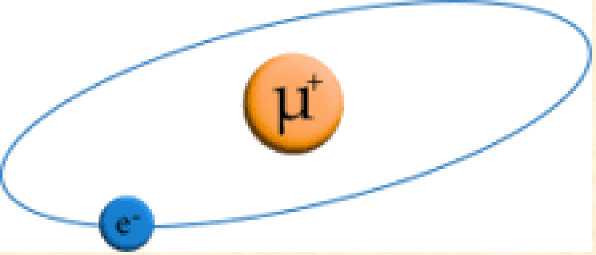

Radiative−Recoil Diagrams

at Order $\alpha^2(Z\alpha)^5$

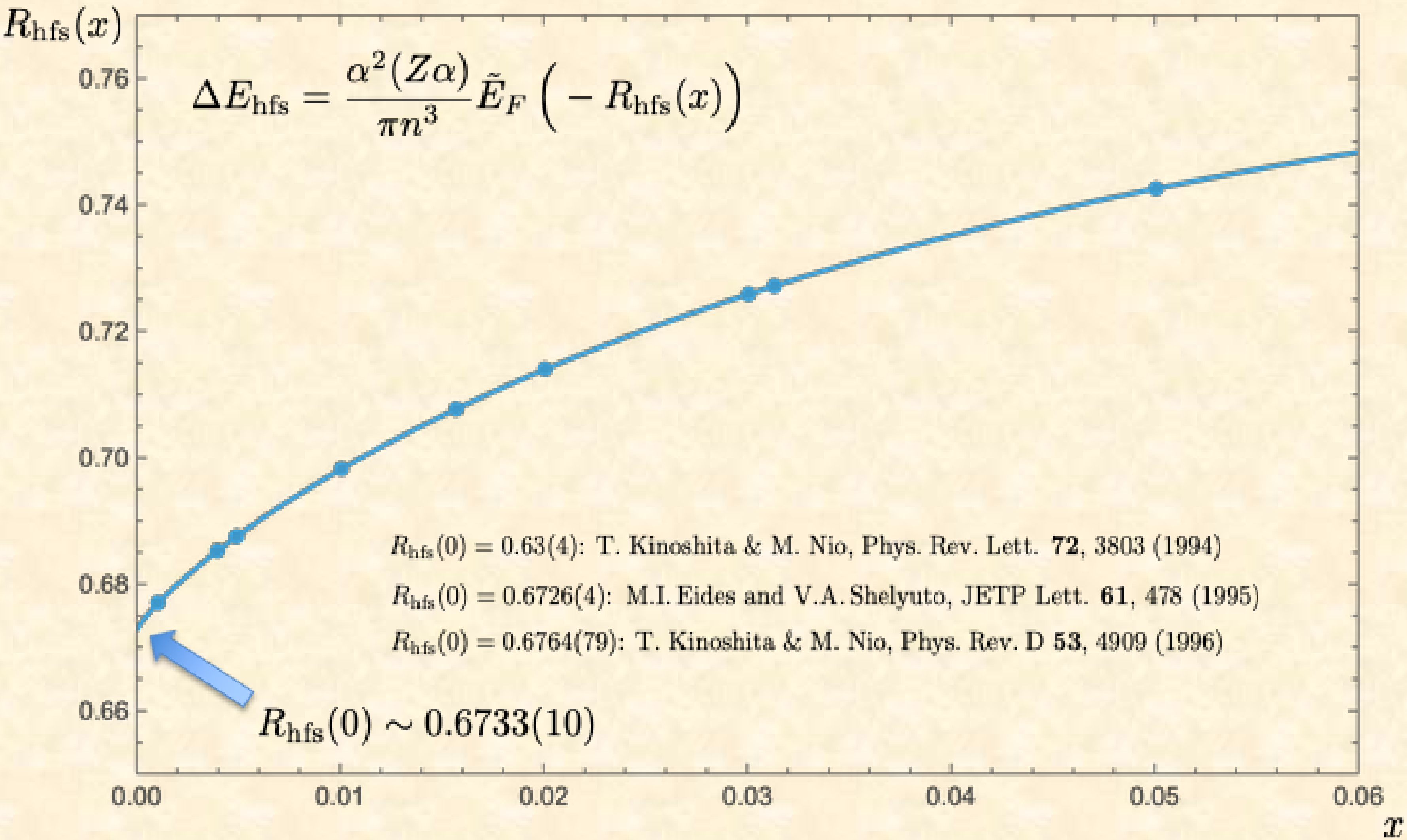

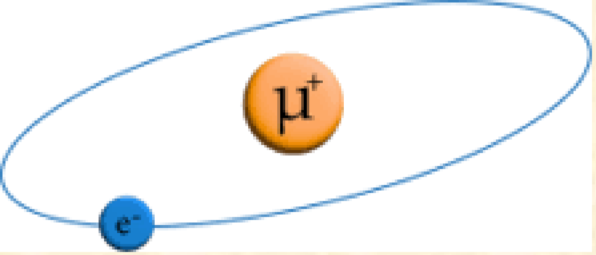

Radiative−Recoil Diagrams at Order $\alpha^2(Z\alpha)^5$

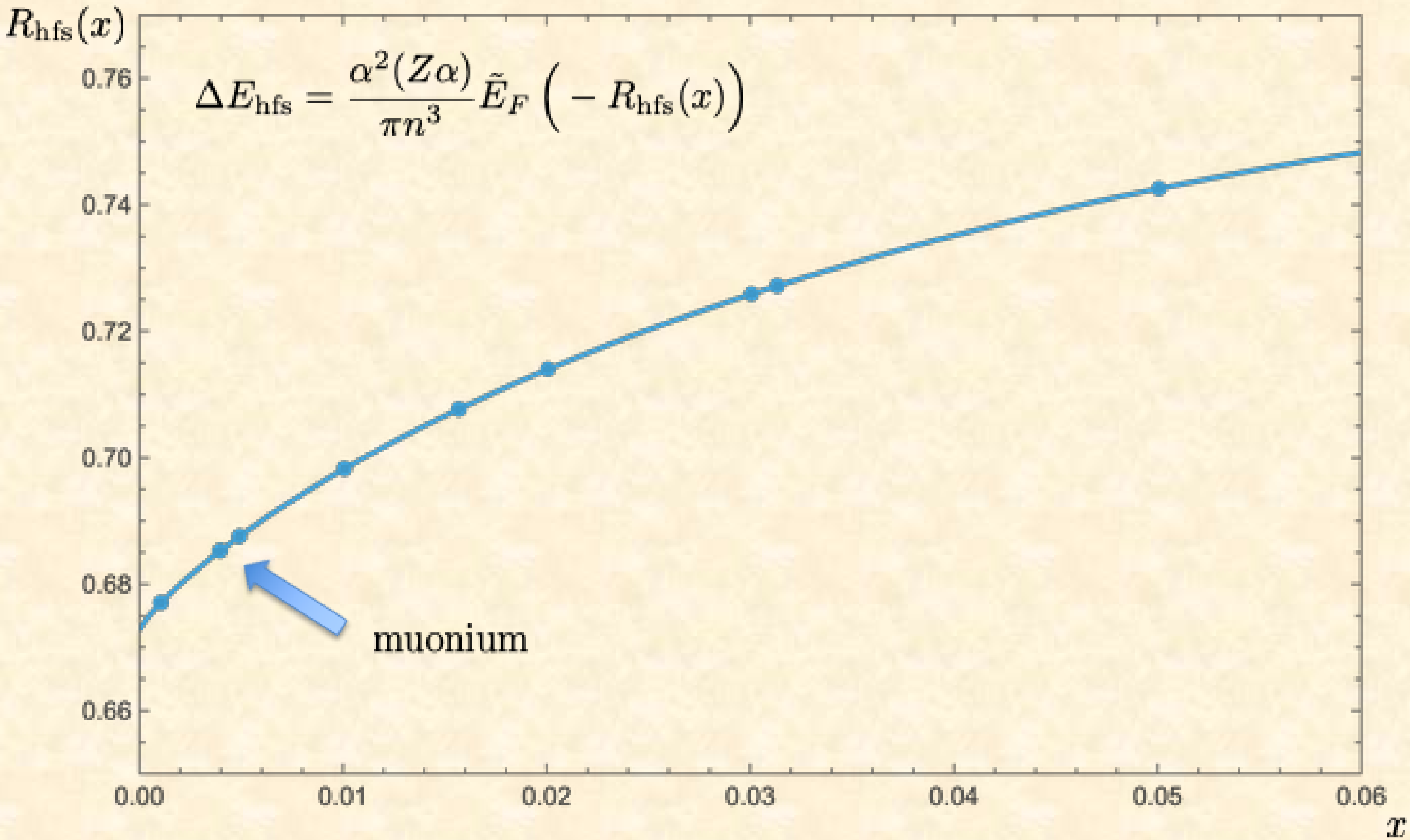

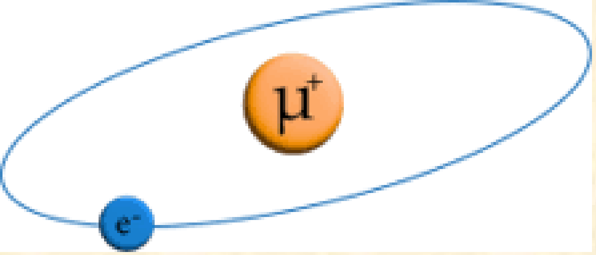

Radiative–Recoil Diagrams at Order $\alpha^2(Z\alpha)^5$

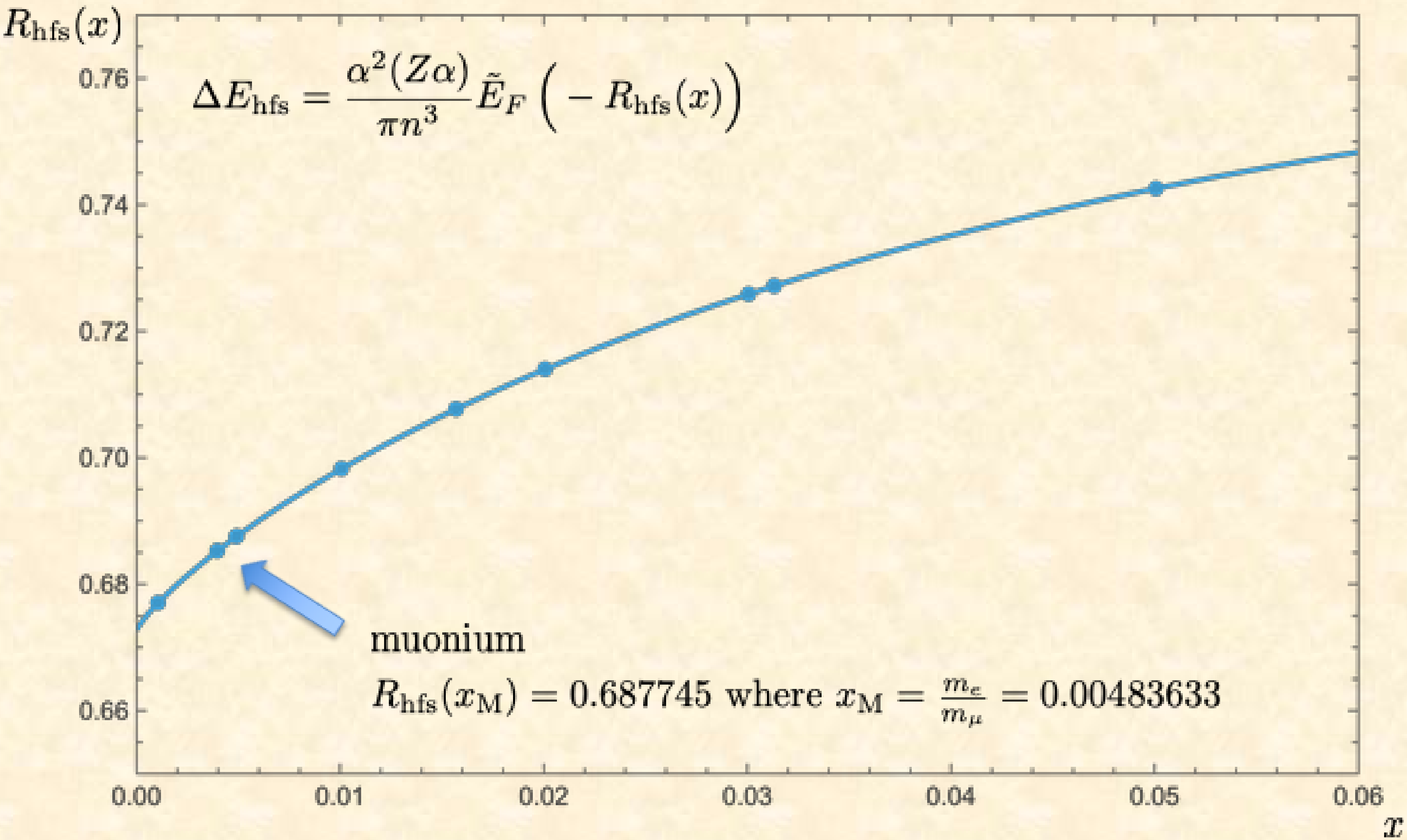

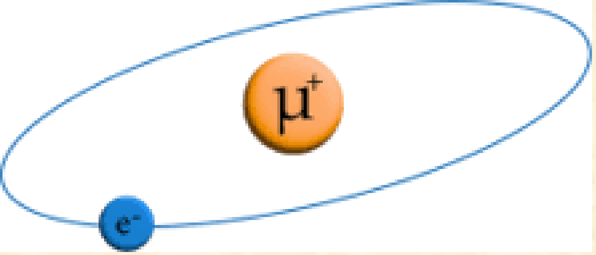

Radiative–Recoil Diagrams at Order $\alpha^2(Z\alpha)^5$

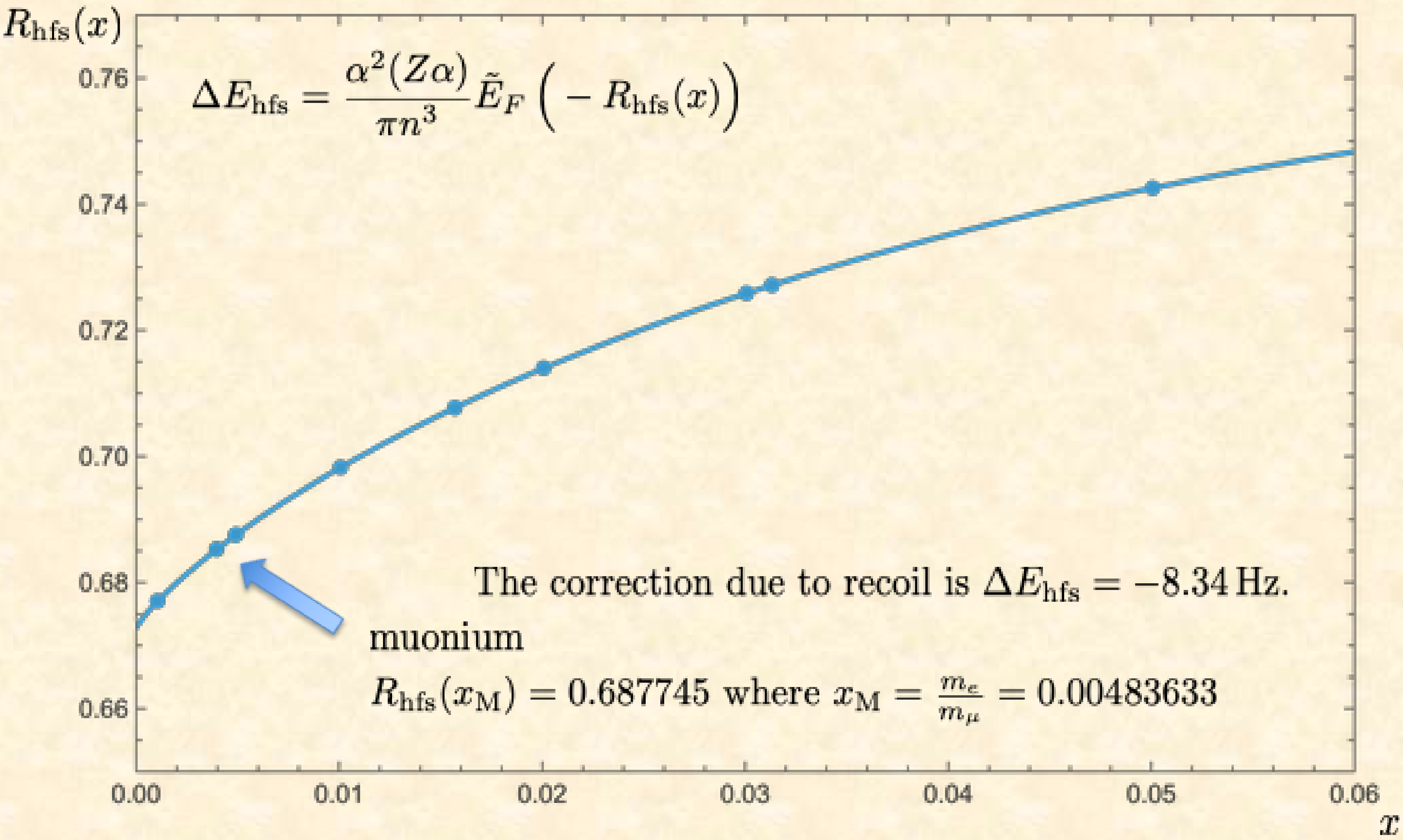

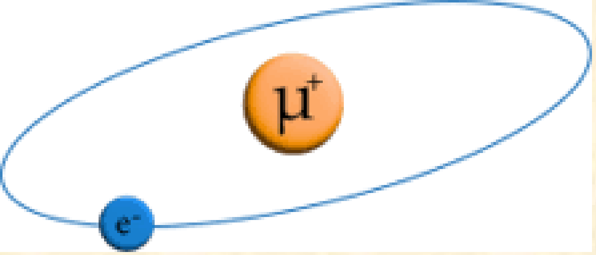

Conclusion

The calculation of recoil and radiative-recoil corrections to muonium and positronium energy levels at order α^7 for arbitrary particle masses is in progress and should reduce the (QED) uncertainties in the muonium energies to a level comparable with expected experimental precisions. Explicit results have been obtained for the radiative recoil contribution of order $m\alpha^2(Z\alpha)^5$.

Modern techniques for the evaluation of Feynman integrals is essential for this work, including the use of Integration by Parts (IBP) for the reduction of many Feynman integrals to a (relatively) small set of ”master integrals”, the use of the “method of differential equations”, along with “expansion by regions”, for the analytic evaluation of the master integrals, and especially the technique of “auxiliary mass flow” and its implementation in the program AMFlow for efficient high-precision numerical evaluation of master integrals.

Thank you!

Greg Adkins
Franklin & Marshall College